Advanced Analysis of Steel Structures

Master Thesis

Written by: Maria Gulbrandsen & Rasmus Petersen

Main Report

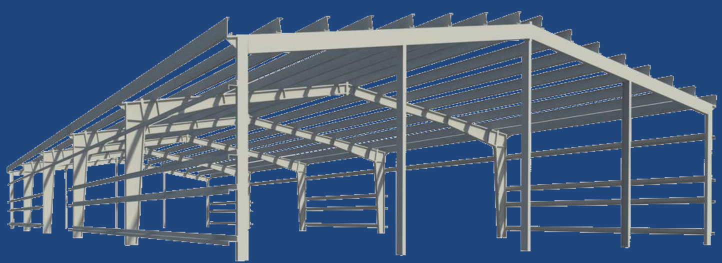

Group B-204d | M.Sc.Structural and Civil Engineering | Aalborg University | 4th Semester | Spring 2013

AALBORG UNIVERSITY
STUDENT REPORT

School of Engineering and Science
Faculty of Engineering and Science
Sohngaardsholmsvej 57, 9000 Aalborg
Telefon: 9940 8530
http://civil.aau.dk

Master Thesis

Title:	*Advanced Analysis of Steel Structures*
Written by:	Maria Gulbrandsen Rasmus Petersen *Group B-204d* Graduate Students School of Engineering and Science M.Sc. in Structural and Civil Engineering
Supervisor:	Lars Pedersen *Associate Professor*
Consultant:	Johan Clausen *Associate Professor*
Project Period:	2013.02.07 - 2013.06.07
Completed on:	Friday the 7th of June 2013
Circulations:	5
Number of Pages:	64
Number of Appendices:	7
Digital Appendices on CD	

Maria Gulbrandsen   Rasmus Petersen

The frontpage pictures are from Freedom Steel [2010] and Made-in-China.com.

Preface

This master thesis is developed at the School of Engineering and Science at Aalborg University by Maria Gulbrandsen and Rasmus Petersen.

A special thanks to our supervisor and examiner Lars Pedersen, Associate Professor at the Department of Civil Engineering for guidance and expertise. Also thanks to our consultant Johan Clausen, Associate Professor at the Department of Civil Engineering for his expertise and help with *Abaqus/CAE*.

The master thesis is a product of the 4th semester of the M.Sc. in Structural and Civil Engineering in the Spring of 2013. The title is *Advanced Analysis of a Steel Frame* and the project has been written in the period of the 7th of February to the 7th of June 2013.

Aalborg, June 2013
Maria Gulbrandsen & Rasmus Petersen

Reading Instructions

References will occur during the main report and these are collected in a bibliography in the back of the report. In the main report are the references listed by the *Harvard Method* so a reference in the text appears as [Last name, Year]. If the reference contains more than one author, the reference is specified by the first last name and then 'et al.'. The reference leads to the bibliography which is listed alphabetically. In the bibliography, books are specified by author, title, edition and possibly publisher. Websites are specified by author, title and the date when the website is downloaded.

Figures and tables are numbered according to the chapter in which they occur. Therefore, the first figure in chapter 7 has number 7.1, the second figure has number 7.2 and so on. Describing text for figures and tables is placed beneath the given figures and tables and the reference is also specified. The figures and tables are made by the project group itself if the reference is not specified. Equations are specified by a number in a bracket and they are numbered like the figures and the tables. Therefore, the first equation in chapter 7 has number (7.1), the second equation has number (7.2) and so on.

Summary

During the latest years, several agricultural buildings and sports arenas in Scandinavia have collapsed due to heavy snowfalls. The loads due to a snowfall result in compression forces and bending moments which are important factors when analysing a steel frame in the ultimate limit state (ULS). These forces and moments can lead to global instability of the steel frame shown as either buckling or lateral torsional buckling failure.

The European design guide Eurocode (EC) presents a number of different methods to use for an analysis of the stability of a steel frame. Some of these methods are more simplifying than others and therefore, the final result - the utilization ratio - is possibly affected by the method chosen for the stability analysis of a steel frame.

This master thesis investigates the behaviour of a pinned supported reference frame constructed in steel due to global instability. The investigation is conducted by comparing the utilization ratios determined, respectively, by the Interaction Formulae given in Clause 6.3.3 and by the General Method given in Clause 6.3.4 in European Standard [2005a].

The Interaction Formulae is directly determining the utilization ratio around either the y or z axis of an element which is subjected to combined bending and axial compression. This method takes also into account both buckling and lateral torsional buckling. The accuracy of this method depends significantly on the assumptions made for the support conditions of the element and the interaction factors which are based on how the moment is assumed to be distributed.

The General Method is based on the determination of two minimum load amplifiers, $\alpha_{\mathrm{ult,k}}$ and $\alpha_{\mathrm{cr,op}}$, related to the in-plane and out-of-plane behaviour of the frame, respectively. This method allows to make use of a *Finite Element Analysis* to determine the two minimum load amplifiers. The *Finite Element Analyis* is conducted by *Abaqus/CAE*, which is an engineering simulation program.

A two-dimensional beam element model is set up for the determination of the in-plane minimum load amplifier, $\alpha_{\mathrm{ult,k}}$, and by using that model a load-displacement curve is drawn to determine $\alpha_{\mathrm{ult,k}}$ by the relationship between a maximum and an actual uniformly distributed line load, q_{max} and q_{actual}, respectively. The out-of-plane minimum load amplifier, $\alpha_{\mathrm{cr,op}}$, is determined by a three-dimensional shell element model where an eigenvalue problem is solved by a buckle analysis performed in *Abaqus/CAE*. The eigenvalue, λ_{cr}, related to the first out-of-plane buckling mode is equal to the minimum load amplifier, $\alpha_{\mathrm{cr,op}}$, for the out-of-plane behaviour of the frame. These two minimum load amplifiers are used to determine the utilization ratio by the General Method.

The utilization ratios determined by the Interaction Formulae and the General Method, respectively, are hereafter compared to see if the methods are giving similar or different results.

In the last part of this master thesis, a parameter study is done to see what influence an effect of a shear wall system, additional fork supports or a change of steel profile can have on the results.

Keywords: *Frame; Steel; Eurocode; Interaction Formulae; General Method; Global Instability; Finite Element Method; Abaqus; Lateral Torsional Buckling; Parameter Study; Numerical Analysis*

Sammendrag

Gennem de seneste år er adskillige landbrugsbygninger og sportshaller i Skandinavien kollapset grundet kraftigt snefald. Belastningerne på grund af et snefald resulterer i trykkræfter og bøjningsmomenter, som er vigtige faktorer, når en stålramme analyseres i brudgrænsetilstanden. Disse kræfter og momenter kan give overordnet instabilitet of stålrammen udtrykt som enten udknæknings eller kipningsbrud.

Den europæiske dimensioneringsnorm Eurocode (EC) præsenterer en række forskellige metoder for at analysere stabiliteten af en stålramme. Nogle af disse metoder er mere forenklende end andre, og derfor er det endelige resultat - udnyttelsesgraden - muligvis påvirket af den valgte metode for stabilitetsanalysen af en stålramme.

Dette kandidatspeciale undersøger opførslen af en fast simpelt understøttet referenceramme konstrueret i stål i forhold til overordnet instabilitet. Undersøgelsen er udført ved at sammenligne udnyttelsesgraderne bestemt henholdsvis ved interaktionsformlen givet i punkt 6.3.3 og ved den generelle metode givet i punkt 6.3.4 i European Standard [2005a].

Interaktionsformlen bestemmer direkte udnyttelsesgraden omkring enten y- eller z-aksen af et element, som er udsat for kombineret bøjning og aksialt tryk. Denne metode tager også højde for både udknækning og kipning. Præcisionen af denne metode afhænger betydeligt af antagelserne for understøtningsforholdene for elementet og interaktionsfaktorerne, som er baseret på, hvordan momentet er antaget at være fordelt.

Den generelle metode er baseret på bestemmelsen af to mindste lastforøgelser, $\alpha_{\mathrm{ult,k}}$ og $\alpha_{\mathrm{cr,op}}$, relateret til henholdsvis opførslen af en ramme i planen og ud af planen. Denne metode tillader at gøre brug af en *Finite Element analyse* til at bestemme de to mindste lastforøgelser. *Finite Element analysen* er udført med *Abaqus/CAE*, som er et ingeniørteknisk simulationsprogram.

En todimensionel bjælkeelementmodel er sat op for bestemmelsen af den mindste lastforøgelse i planen, $\alpha_{\mathrm{ult,k}}$, og ved brug af den model er en arbejdskurve optegnet til at bestemme $\alpha_{\mathrm{ult,k}}$ ved forholdet mellem henholdsvis en maksimal og en aktuel jævnt fordelt linjelast, q_{max} og q_{actual}. Den mindste lastforøgelse ud af planen, $\alpha_{\mathrm{cr,op}}$, er bestemt ved en tredimensionel skalelementmodel, hvor et egenværdiproblem er løst ved en buleanalyse udført i *Abaqus/CAE*. Egenværdien, λ_{cr}, relateret til den færste udknækningstilstand ud af planen er lig med den mindste lastforøgelse, $\alpha_{\mathrm{cr,op}}$, for opførslen af rammen ud af planen. Disse to mindste lastforøgelser er brugt til at bestemme udnyttelsesgraden med den generelle metode.

Udnyttelsesgraderne bestemt ved henholdsvis interaktionsformlen og den generelle metode er herefter sammenlignet for at se, om metoderne giver tilsvarende eller forskellige resultater.

I den sidste del af dette kandidatspeciale er et parameterstudie udført for at se, hvilken indflydelse effekten af skivevirkning, supplerende gaffellejer eller en ændring af stålprofil kan have på resultaterne fra de to Eurocode-metoder.

Stikord: *Ramme; Stål; Eurocode; Interaktionsformel; Generel metode; Instabilitet; Finite Element Metode; Abaqus; Fri kipning; Bunden kipning; Parameterstudie; Numerisk analyse*

Symbols

Latin Upper Case Letters

ΔM_{Ed}	additional moment from shift of the centroid of the effective area A_{eff} relative to the center of gravity of the cross-section
M_{cr}	elastic critical moment for lateral torsional buckling
$M_{\mathrm{y,Rd}}$	design values of the resistance to bending moment, y-y axis
$M_{\mathrm{z,Rd}}$	design values of the resistance to bending moment, z-z axis
N_{cr}	elastic critical force for the relevant buckling mode based on the gross cross-sectional properties
N_{Ed}	design normal force
N_{Rd}	design values of the resistance to normal forces
V_{Ed}	design shear force

Latin Lower Case Letters

E	modulus of elasticity
f_{y}	yield strength
G	shear modulus
k_{c}	correction factor for moment distribution
k_{yy}	interaction factor
k_{yz}	interaction factor
k_{zy}	interaction factor
k_{zz}	interaction factor

Lower Case Greek Letters

α	imperfection factor for lateral buckling
α_{LT}	imperfection factor for lateral torsional buckling
$\alpha_{ult,k}$	minimum load amplifier of the design loads to reach the characteristic resistance of the most critical cross section
$\alpha_{cr,op}$	minimum load amplifier of the design loads to reach the elastic critical resistance with regard to lateral or lateral torsional buckling
β	correction factor for the lateral torsional buckling curves for rolled sections
γ_{M0}	partial factor for resistance of cross-section whatever the class is
γ_{M1}	partial factor for resistance of members to instability assessed by member checks
χ	reduction factor due to flexural bucking
χ_{LT}	reduction factor due to lateral torsional buckling
$\overline{\lambda}$	non-dimensional slenderness
$\overline{\lambda}_{LT}$	non-dimensional slenderness for lateral torsional buckling
ψ	ratio of moments in segment

Upper Case Greek Letters

Φ	value to determine the reduction factor χ
Φ_{LT}	value to determine the reduction factor χ_{LT}
Σ	sum

Abbreviations

C-S	cross-section
EC	Eurocode
EHF	equivalent horisontal force
ULS	ultimate limit state

Table of Contents

1 Introduction

In the recent years, there has been a number of collapses of different sport arenas and agricultural buildings in Scandinavia due to heavy snowfall. A lot of research and statistics have been produced in order to uncover the reason for the collapses and if there is anything that can be improved [Solberg, 2011] [Andersen and Petersen, 2010].

In general, steel frames are commonly used in warehouses, sport centers, in agricultural and large industry buildings. Some examples of the use of the frames in structures can be seen in Figure 1.1.

Figure 1.1: Example of steel frames [Autobaler][Steltech-Structural].

Steel frames are usually the choice when constructing a larger building that needs a big open space because of the economical aspect and efficiency of building a single-storey unit. However, a problem that might occur is when designing for a cost effective solution the slenderness may be decreased, that in the end may contribute to an instability of the entire structure.

A typical frame will in ultimate limit state (ULS) have compression forces and bending moments that are of big concern. The reason for this is that they may cause one element to buckle and deform. Because the elements are connected to each other, this may result in a deformation of the neighbouring element which in the end may lead to severe deformations and instability of the entire system of the frame. It is therefore important to know about the critical conditions when designing a frame.

1.1 Definition of a Frame

There are two main configurations of a frame; flat-roofed portal frame and pitched-roof portal frame. An illustration of the two different frames can be seen in Figure 1.2.

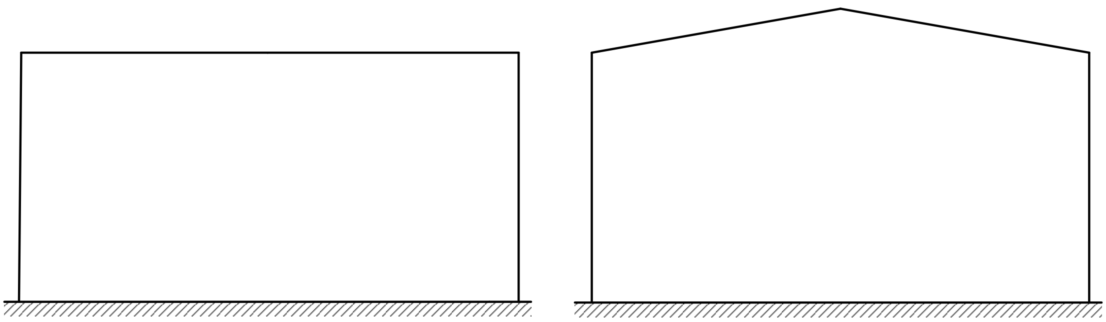

Figure 1.2: Sketch of two different frames; flat-roofed portal frame on the left hand side and pitched-roof portal frame to the right hand side.

1.2 Instability of a Frame

Instability of a frame is of outmost concern. Mainly because instability of frames has lead to several collapses of structures, see Figure 1.3

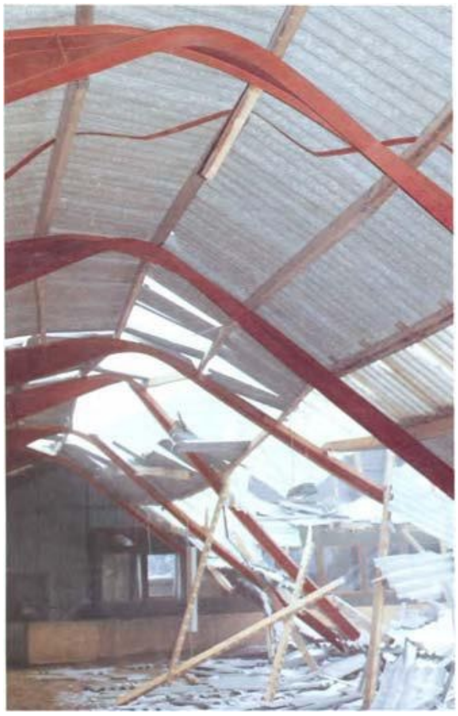

Figure 1.3: Collapse due to lateral torsional buckling [BYG-ERFA].

Instability may occur in members where compression stresses exist, and instability is most common for slender members. The result is buckling of the member and will in the end lead to failure of the structure. Instability is the result of different buckling modes, and the most common buckling modes are:

- Flexural Buckling
- Torsional Buckling
- Flexural Torsional Buckling
- Lateral Torsional Buckling

Flexural Buckling:

According to Eurocode-resources.com, flexural buckling is a phenomena that occurs about the axis of the highest slenderness ratio and the smallest radius of gyration. It can happen in any member subjected to compression, which in the end will lead to deflection of the member. An illustration of the flexural buckling can be seen in Figure 1.4.

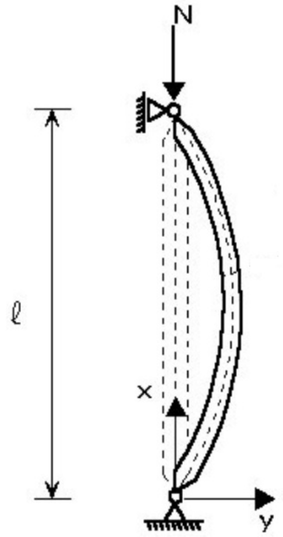

Figure 1.4: Flexural buckling of a column [Ljubljana University, a].

Torsional Buckling:

Torsional buckling is a form of buckling occurring about the longitudinal axis of a member, where the center of the member remains straight while the rest of the section rotates. An illustration of this can be seen in Figure 1.5. As stated by Ljubljana University [b] “torsional buckling can only properly occur when the shear center and the centroid of the cross-section are coincident”.

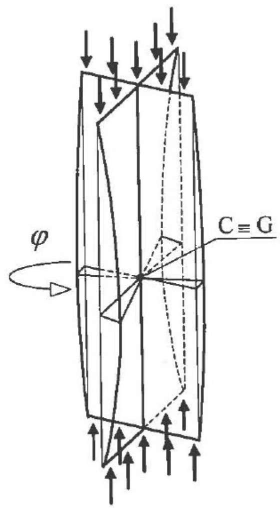

Figure 1.5: Illustration of torsional buckling [da Silva and et al, 2010].

Flexural Torsional Buckling:

According to da Silva and et al [2010], it is so that “flexural torsional buckling consists of the simultaneous occurrence of torsional and bending deformations along the axis of the member”. An illusration of this can be seen in Figure 1.6. In Connections.org, it is stated that flexural torsional buckling mostly occurs in channels and structural tees.

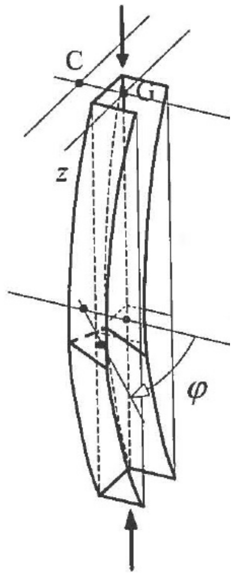

Figure 1.6: Illustration of flexural torsional buckling [da Silva and et al, 2010].

Lateral Torsional Buckling:

Lateral torsional buckling is as stated in da Silva and et al [2010] "characterized by lateral deformation of the compressed part of the cross-section". In an I-section, the compressed part will be one of the flanges. As a part of the member will behave under compression, it will also simultaneously have one continuously restrained by the part of the section in tension. This will result in a deformation of the cross-section where both lateral and torsion buckling is included. Hence the name lateral torsional buckling [da Silva and et al, 2010].

There is a difference between constrained and unconstrained lateral torsional buckling as they will behave differently under the buckling process. It is understood that with constrained lateral torsional buckling means that a point of the member is restrained against deformations across the length of the member. This means that the axis of rotation is made fixed, which is where the member buckles around, see Figure 1.7 [Bonnerup and et al., 2009].

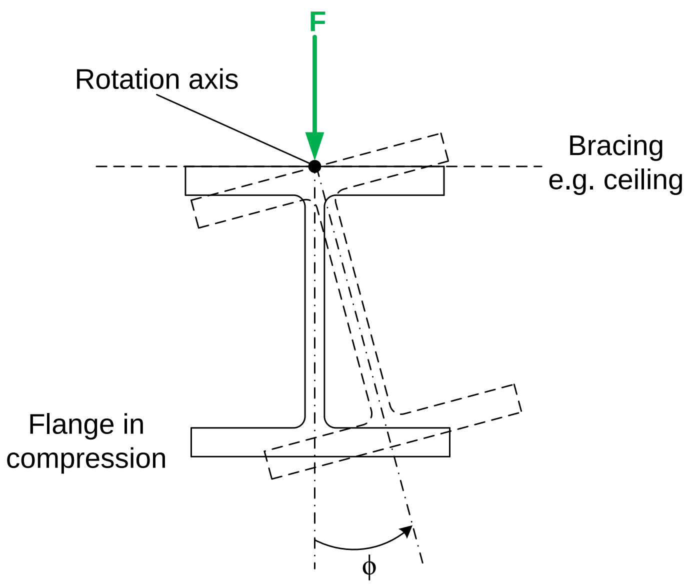

Figure 1.7: Constrained lateral torsional buckling [Bonnerup and et al., 2009].

With unconstrained lateral torsional buckling, the axis of rotation is not given in advance, and it is therefore more complicated to determine the capacity, as it is dependent of the members internal balance at buckling, see Figure 1.8.

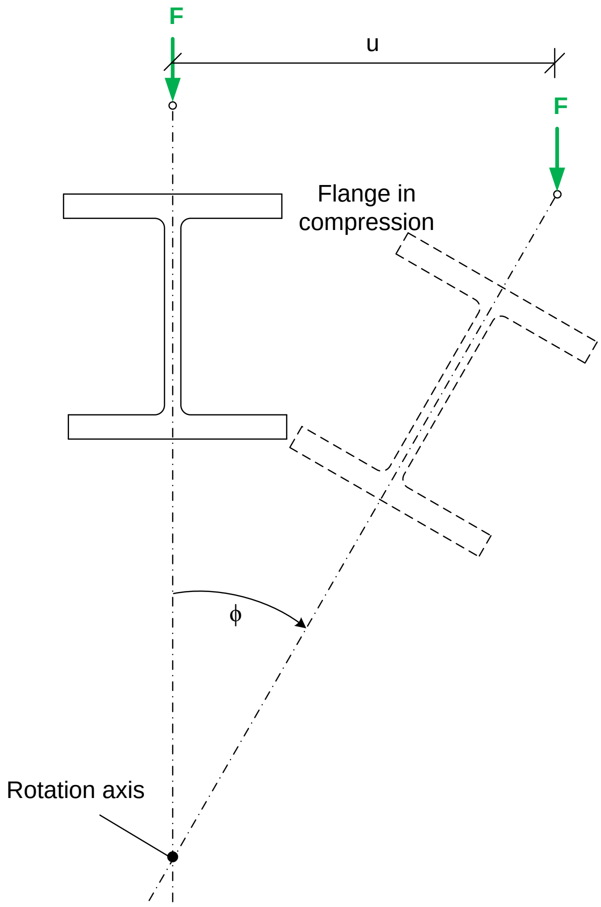

Figure 1.8: Unconstrained lateral torsional buckling [Bonnerup and et al., 2009].

The point of application in respect to the load will influence the elastic critical moment of a member. As stated in da Silva and et al [2010] “a gravity load applied below the shear centre C (that coincides with the centroid, in case of doubly symmetric I or H sections) has a stabilizing effect ($M_{\mathrm{cr},1} > M_{\mathrm{cr}}$), whereas the same load applied above this point has a destabilizing effect ($M_{\mathrm{cr},2} < M_{\mathrm{cr}}$)”. This is illustrated in Figure 1.9.

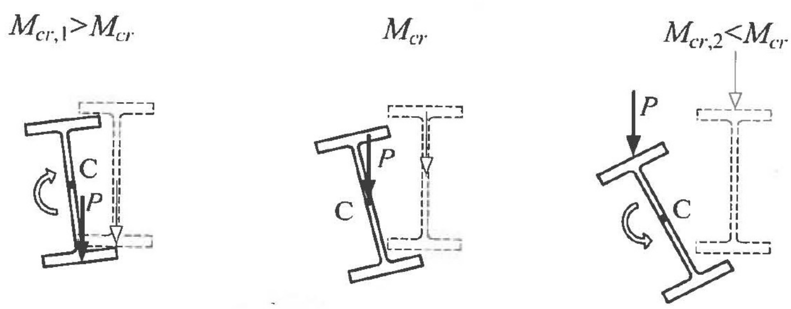

Figure 1.9: Effect of the point of load’s application [da Silva and et al, 2010].

1.2.1 Prevention of Instability

In order to prevent instability and out-of-plane buckling, it is common to use adequate bracings. The bracings must as stated in da Silva and et al [2010] "provide effective restraint to lateral displacements of the compressed flange about the minor axis of the cross-section, and should prevent the rotation of the cross-section about the longitudinal axis of the member". There are three different kinds of bracings that can contribute to prevent the out-of-plane buckling. These are:

- Lateral bracings - prevents transverse displacements of the compression flange
- Torsional bracings - prevents rotation of a cross-section around its longitudinal axis
- Partial bracings - bracing of the tension flange, which however does not fully prevent out-of-plane buckling, but is equivalent to an elastic support

There are, in addition to bracings, checks that can be done in the Eurocode (EC). The checks will show whether buckling and lateral torsional effects may be ignored for the member. The check of the buckling effects takes the slenderness of the member into account in addition to the relationship between the occurring normal force and the critical normal force. In regard of lateral torsional buckling, the slenderness of the member is checked in addition to the relationship between the occurring moment and the critical moment for the section.

1.3 Calculations of a Frame

Nowadays, there are given two different methods by European Standard [2005a] to calculate a frame and to check the frame if it is able to withstand the load applied without any failure. In Section 6.3.3 in European Standard [2005a], Interaction Formulae is introduced. The method is used to see if a member subjected to combined bending and axial compression does not reach a utilization over 100%. However, Interaction Formulae can only be applied when the cross-section of a member is constant. Today, it is most likely that Interaction Formulae is used even if the cross-section is not constant, as it is easier to use this method and that it is recognized by most engineers. Eurocode has however come up with another method called the General Method, given in Section 6.3.4 in European Standard [2005a]. This can be used even if the cross-section of a member is not constant. The general method implies the use of *Finite Element Method* (FEM) to verify a load amplifier of the design load to reach the characteristic resistance of the most critical cross-section and the minimum amplifier for the in-plane design loads to reach the elastic critical resistance. In this way, the method allows for a check to see if the forces and moments acting on the frame can be resisted by the members of the frame by the use of FEM.

1.4 Aim of the Project

The aim of the project is to examine a frame with respect to instability due to different failure modes such as flexural buckling and lateral torsional buckling. In order to verify the different instabilities of the frame, different methods are used. Two methods from European Standard [2005a] are used where an elastic and plastic analysis is conducted. Then, a third more advanced method by the use of FEM is performed. The different methods are then compared to each other and analysed further to see their limitations and what they take into account. Then, a parameter study is conducted to see how different parameters will influence the calculations of the method and the instability of the frame. In the end of the project, a conclusion of the parameter study and the differences of the two EC methods is given.

In the beginning of the project, a reference frame of a simple flat-roofed portal frame will be investigated. The frame will have profiles given by an assessment of Interaction Formulae in the EC. The loads for the calculation of the structure are based on a real, but simplified, assessment of loads and load combinations given by the EC. It is also so that EC gives two different ways of checking the capacity of a steel frame. These equations will be a part of a further study in order to investigate how these are used for the capacity of a steel frame. After an investigation of the different methods, a parameter study is done. The parameter study will include the reference frame with unconstrained flanges, with different profiles and with additional fork supports. In addition, the effect of shear wall is also analysed. In the end of the project, comparison and conclusions will be made in order to understand the different impacts of these parameters. A flow chart of the the contents of the project can be seen in Figure 1.10.

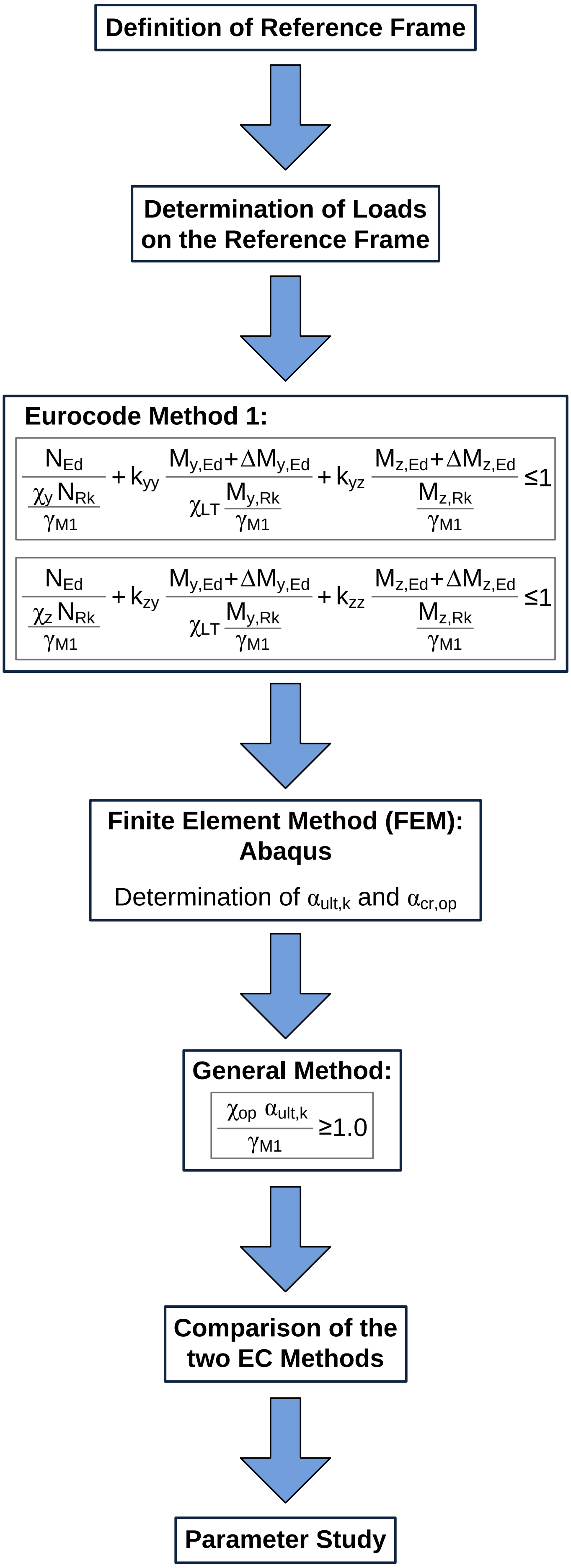

Figure 1.10: Flow chart of the contents of the project report.

1.5 Method

In order to achieve the aim of the project and be able to understand the behaviour of a steel frame, a literature study is made to understand the behaviour of a steel frame and the parameters influencing this. The focus is on literature explaining the different mechanisms of a frame, but also on Eurocode 3 part 1-1, where detailed suggestions on how to calculate a steel frame are presented. In addition, the different Eurocodes containing loads such as imposed load, snow load and wind load have been simplified but ensured to be a good estimate of the loads in a further analysis of the frame.

In order to make a reasonable comparison between the analytical solution based on the equations in the EC and the models made in *Abaqus/CAE* , a further understanding of *Abaqus/CAE* is also made. In this thesis *Abaqus/CAE* is used to analyse a frame numerically by the *Finite Element Method* (FEM). In addition, a parameter study is also conducted in order to elicit the behaviour of a steel frame.

1.6 Scope and Limitations

The scope of the project is to look at the two different expressions given by European Standard [2005a] and be able to understand their assumptions and what they take into consideration. FEM is also used as a part of the General Method in EC and as a more advanced analysis of the frame. It is therefore necessary to be able to understand the basis of FEM and how the software *Abaqus/CAE* applies FEM in order to analyse a frame. The scope is also to be able to look at different stability problems and failure modes of a frame, and be able to understand these mechanisms and the significant parameters influencing it. In addition, the parameter study is made to get an overview of the similarities and differences between the two methods from the EC, and to see the correlation the different parameters have to determine the behaviour of the frame.

There are a number of different parameters which are well suited for an analysis of a frame, but because of the extent and complexity of frame, only some parameters has been chosen.

In this project, the basic geometry of the frame will not be changed as some parameters need to be fixed through out the analysis. In this way, it is possible to see if there are other parameters influencing a frame besides the width, depth and height of the structure.

2 Reference Frame

The following chapter contains explanations for the choices made before using the two Eurocode methods to investigate the instability of a frame. In addition, different assumptions and considerations about the frame design are given.

2.1 Dimensions

The dimensions of the reference frame constructed in steel can be seen in Figure 2.1. The dimensions are in accordance to how a steel frame is constructed normally in real life, and these will not be varied during this project report.

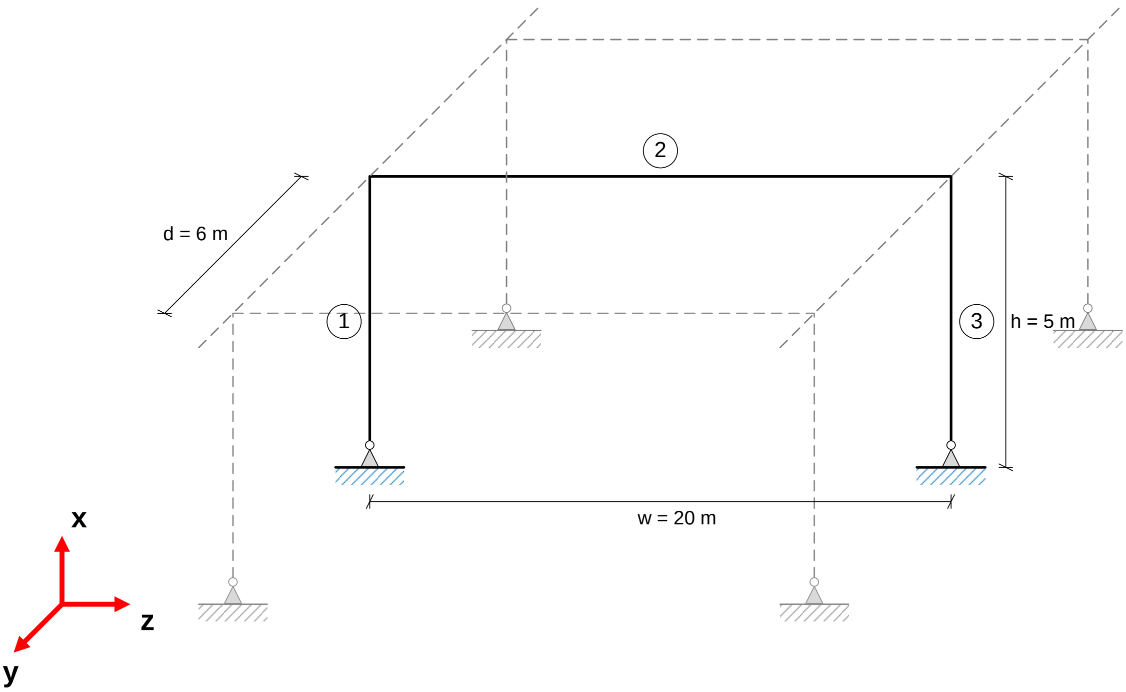

Figure 2.1: Illustration of the reference frame in a construction.

The circles with a number placed inside in Figure 2.1 and 2.2 (1, 2 and 3) are used as references for the different elements which in total form the reference frame.

2.2 Statical Model

A reference frame is assumed, and and the statical model of it is shown on Figure 2.2.

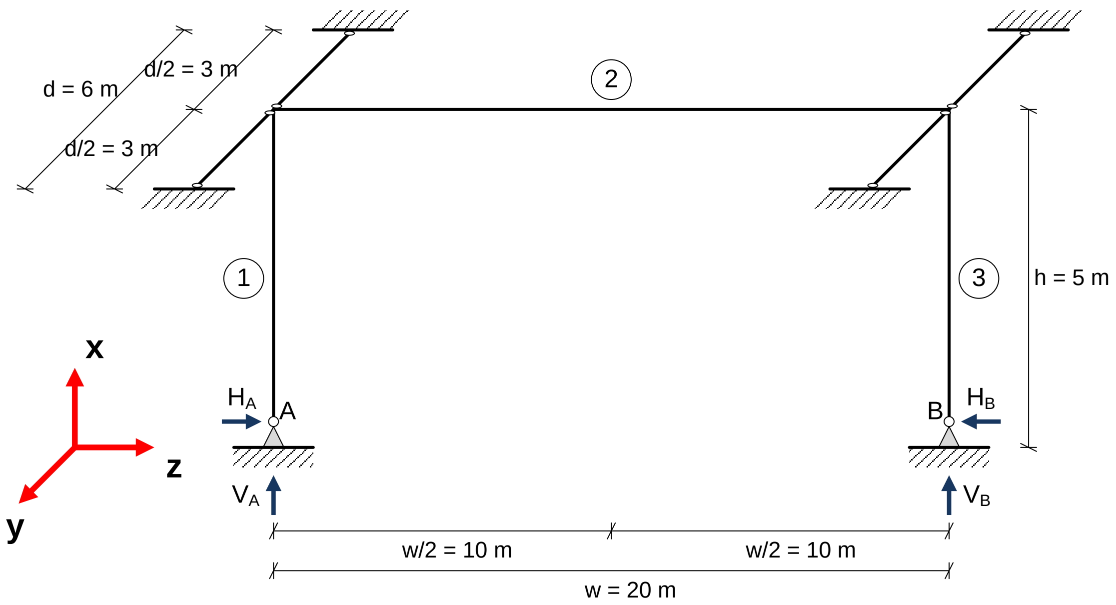

Figure 2.2: Statical model of the reference frame.

The frame is supported by pinned supports which makes it one time statically indetermined because there is one more reaction, r, than equilibrium equations, e ($r = 4$, $e = 3$). Out of the plane, bracings are used to connect the frames which make them pinned supported in that direction as well as seen in Figure 2.2.

The frame is designed as a steel structure where the elements are assumed to have a constant stiffness ($E\,I =$ constant) depending on in which direction, the investigation is done.

2.3 Profiles

For this project, a HE320A steel profile has been chosen for the reference frame. The real cross-section of a HE320A steel profile is shown on the left hand side in Figure 2.3 while the cross-section assumed in this project report is shown on the right hand side in Figure 2.3. The reason for this assumption is that the profile in Abqus/CAE will be according to the profile shown on the right hand side in Figure 2.3. This means that for the analytical assessment, the profile will also assumed to have this cross-section.

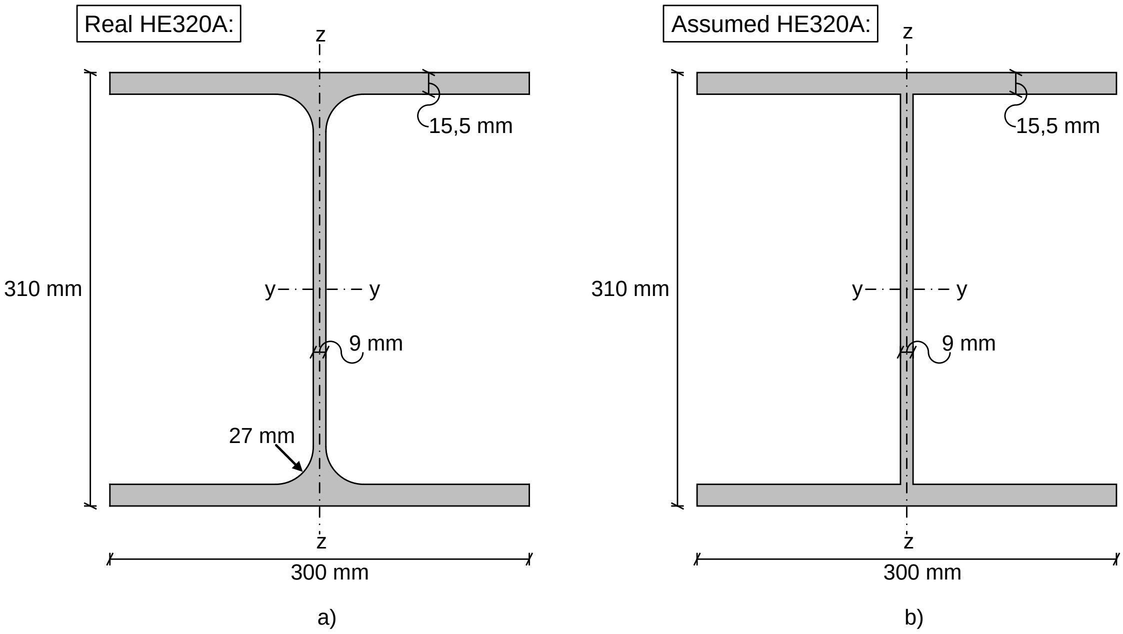

Figure 2.3: Steel profile assumption - a) Real HE320A steel profile; b) Assumed HE320A steel profile.

2.4 Material Properties

It has been chosen to work with a frame consisting of steel S235. The general material properties for construction steel S235 are given in Table 2.1. The behaviour of the steel is considered perfect elastic-plastic, and the stress-strain relationship is shown in Figure 2.4. It is the Von Mises platicity which is used. The diagram shown on the left hand side is the real behaviour of steel while the diagram shown on the right hand side is the assumed behaviour used in this project report.

Description	Symbol	Value	Unit
Yield Strength of Construction Steel S235	f_y	235	[MPa]
Modulus of Elasticity	E	210000	[MPa]
Shear Modulus	G	81000	[MPa]
Density	ρ	7850	[kg/m^3]
Poisson's Ratio	ν	0.3	[-]

Table 2.1: Material properties for construction steel S235.

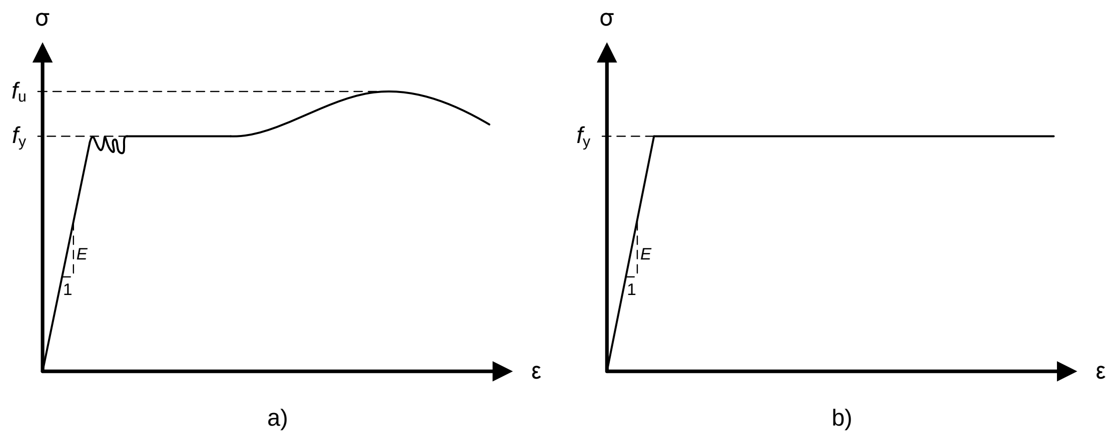

Figure 2.4: Stress-strain relationship - a) Real behaviour; b) Perfect elastic-plastic behaviour.

The partial factor, γ_{M1}, for resistance of members to instability assessed by member checks is determined on the basis of the control class which is chosen to be normal ($\gamma_3 = 1.00$). The calculations are done on laterally loaded columns and elements possibly affected by lateral torsional buckling and because of that, the partial factor, γ_{M1}, becomes equal to 1.20. In addition, it is so that for cross-sectional checks, the partial factor, γ_{M0}, becomes equal to 1.1 as the control class is normal.

2.5 Configurations of a Frame

The reference frame is assumed to be detached from the total structural system of frames representing a kind of building. However, the reference frame is assumed to have fork supports in th the corners of the frame. This means that there will not be any shear wall system effect as shown in case a) in Figure 2.5. This assumption affects the stability of the frame because the reference frame is only supported in the corners.

In case b) in Figure 2.5, the reference frame is shown with a shear wall system effect whereby the frame is supported out-of-the-plane by some kind of cladding. This means that the stability of the frame is increased because the cladding is assumed to support the entire frame out-of-the-plane.

The part of Figure 2.5 called c) illustrates a way to support the reference frame out-of-the-plane. Here, it is done by additional fork supports which make the elements of the frame possibly exposed to unconstrained lateral-torsional buckling with a reduction of the buckling length.

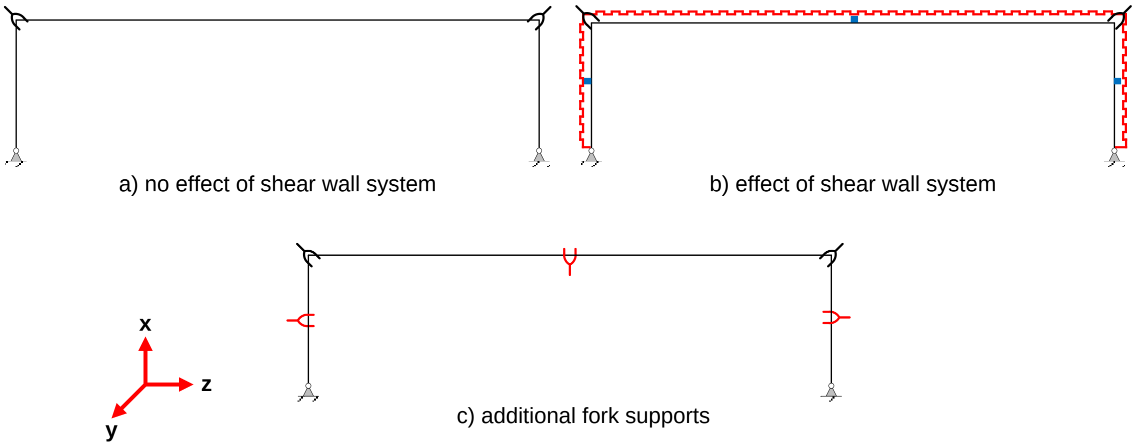

Figure 2.5: Effect of Shear Wall System - a) No effect of shear wall system; b) Effect of shear wall system; c) Additional fork supports.

If the reference frame is modelled as in case b) or c), the situation regarding the lateral torsional buckling changes because the supporting conditions of the elements forming the reference frame change. Thereby, the elements switch from being possibly exposed to unconstrained to constrained lateral torsional buckling.

3 Loads

Normally, a frame is exposed to the following four kinds of load types:

- Permanent Loads
- Snow Load
- Wind Loads
- Imposed Load

In this chapter, a quick assessment and explanation of the determined loads will be done. In addition, the load combinations will be stated so that in the end, the final load scenario of the frame is found.

3.1 Permanent Loads

The permanent load of the considered frame is its self-weight. The self-weight of the frame is calculated for the different profiles used in the analysis. The permanent load of the frame is given in Table 3.1. It is chosen to have a HE320A profile on the frame, where in Appendix B, an example of how the right profile is found can be seen. HE320A is a profile that satisfies the equations of method 1 in the Eurocode (see eq. 4.1 and 4.2 in section 4.1).

Profile	Weight	Permanent load
HE320A	97.6 kg/m	0.957 kN/m

Table 3.1: Self-weight of HE320A steel profile.

In addition, the load on the roof of the structure is taken as a light weight roof of 0.50 kN/m^2 [Lett-Tak Systemer AS]. Also, the cladding of the structure needs to be taken into consideration. It is therefore chosen that the load of the cladding will be the same as for the roof (0.50 kN/m^2).

3.2 Snow Load

The snow load is a variable load as the loading is not constant during the year. The snow load will in general vary depending on the location of the structure, the slope angle of the roof, contribution and interference of other roofs and contribution and drifting at projections and obstructions.

In this project, the characteristic snow load is calculated to be 0.72 kN/m^2. The calculations are done by following European Standard [2007a]. The calculations are based on a frame with a slope angle of 0°, as this is the most critical case. In addition, the frame is assumed to have a location of normal topography. Most commonly, sports arenas, industry and agricultural buildings are placed in more remote/outlying locations, which means that the topography will be windswept. However, this will result in a lower snow load, and it will therefore not be applicable in this case.

3.3 Wind Loads

The wind load is calculated based on European Standard [2007b]. The wind has been calculated from the west direction as the highest wind load will occur in this direction. Also, the frame is subjected to wind during the whole year, giving it the most critical seasonal factor. The terrain category is chosen to be of category II, corresponding to a location at the countryside, meaning that the frame may have a few obstacles like trees and buildings around. This corresponds to the same topography as used in the snow load calculation.

A simplification of the wind load has been made in regards of the wind pressure on the roof and the internal pressure. The calculations show both a suction on some parts of the roof and pressure on other parts. The different parts are depended on the width of the structure. A simplification is therefore made to ignore wind loads on the roof and the internal pressure.

The calculations of characteristic wind load shows a windward pressure of 0.49 kN/m^2 and a negative leeward pressure of -0.21 kN/m^2. This is also illustrated in Figure 3.1.

3.4 Imposed Load

The imposed load is taken from section 6.3.4 in European Standard [2002] where category H is classified as “roofs not accessible except for normal maintenance and repair” [European Standard, 2002], which will be the case for the frame. In the national annex, a value of 0 kN/m^2 is given to this category, meaning that the frame will not have any imposed load.

3.5 Summary of Loads

Self-weight	Roof	Cladding
0.957 kN/m	0.5 kN/m^2	0.5 kN/m^2

Table 3.2: Permanent loads.

Snow load	Wind load, windward	Wind load, leeward	Imposed load
0.72 kN/m^2	0.49 kN/m^2	-0.21 kN/m^2	0 kN/m^2

Table 3.3: Summary of the variable loads.

The load situation on the frame is illustrated in Figure 3.1.

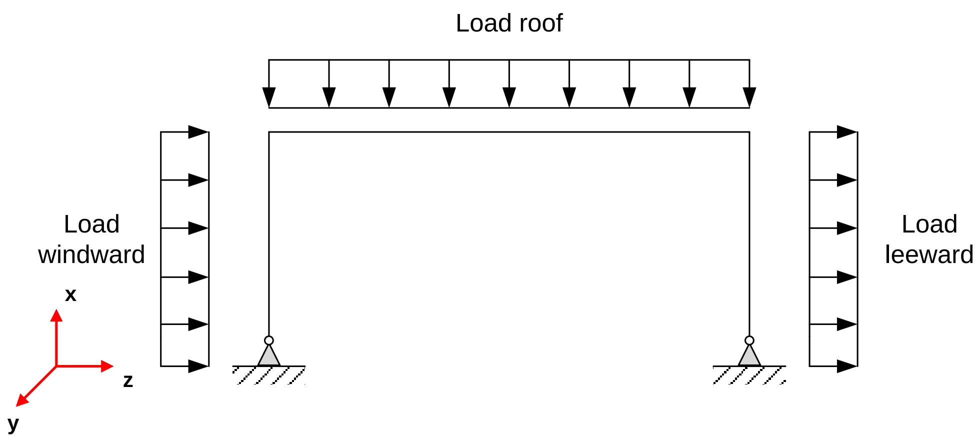

Figure 3.1: Principle sketch of loads on a frame.

3.6 Load Combinations and Loads on the Reference Frame

The following equation is used for calculating the load combination:

Permanent actions	Leading variable	Accompanying variable
$\xi\ K_{\mathrm{FI}}\ \gamma_{\mathrm{Gj,sup}}\ G_{\mathrm{kj,sup}}$	$K_{\mathrm{FI}}\ \gamma_{\mathrm{Q,1}}\ Q_{\mathrm{k,1}}$	$K_{\mathrm{FI}}\ \gamma_{\mathrm{Q,i}}\ \psi_{0,\mathrm{i}}\ Q_{\mathrm{k,i}}$

Table 3.4: Design values of actions (STR/GEO) [European Standard, 2005b].

$G_{\mathrm{kj,sup}}$	Upper/lower characteristic value of permanent action j	[kN/m]
$Q_{\mathrm{k,1}}$	Characteristic value of the leading variable action 1	[kN/m^2]
$Q_{\mathrm{k,i}}$	Characteristic value of the accompanying variable action i	[kN/m^2]
ξ	Reduction factor, given in Table 3.5	[-]
K_{FI}	Consequence class factor, given in Table 3.5	[-]
$\gamma_{\mathrm{Gj,sup}}$, $\gamma_{\mathrm{Q,i}}$	Partial factors, given in Table 3.5	[-]
$\psi_{0,\mathrm{i}}$	Factor for combination value of a variable action i, given in Table 3.5	[-]

Description	Symbol	Value
Reduction factor	ξ	1.0
Consequence class factor for CC2	K_{FI}	1.0
Partial factor for permanent action j in calculating upper/lower design values	$\gamma_{\mathrm{Gj,sup}}$	1.0
Partial factor for variable action i	$\gamma_{\mathrm{Q,i}}$	1.5
Factor for combination value of a variable action i	$\psi_{0,\mathrm{i}}$	0.3

Table 3.5: Different safety factors given in European Standard [2005b].

From this, the following load combination factors can be calculated.

Permanent load	Leading variable	Accompanying variable
$1.0 \cdot 1.0 \cdot 1.0 \cdot G_{\mathrm{kj,sup}}$	$1.0 \cdot 1.5 \cdot Q_{\mathrm{k,1}}$	$1.0 \cdot 1.5 \cdot 0.3 \cdot Q_{\mathrm{k,i}}$

Table 3.6: Load combination factors.

When the load combination factors are used, the value of the loads can be calculated. The different load combinations that can be used is when snow is dominant and when wind is dominant. When the wind is dominant, no snow load is applied. The loads are calculated for a span of 6 m (see chapter 2).

Dominant load	Permanent load	Leading variable
Snow	$1.0 \cdot (0.957\ \mathrm{kN/m} + (0.5\ \mathrm{kN/m^2} \cdot 6\ \mathrm{m}))$	$1.5 \cdot (0.72\ \mathrm{kN/m^2} \cdot 6\ \mathrm{m})$
Wind	$1.0 \cdot (0.957\ \mathrm{kN/m} + (0.5\ \mathrm{kN/m^2} \cdot 6\ \mathrm{m}))$	$1.5 \cdot (0.49\ \mathrm{kN/m^2} \cdot 6\ \mathrm{m}\ )$

Dominant load	Accompanying variable	Accompanying variable 2
Snow	$0.45 \cdot (0.49\ \mathrm{kN/m^2} \cdot 6\ \mathrm{m})$	$0.45 \cdot (-0.21\ \mathrm{kN/m^2} \cdot 6\ \mathrm{m})$
Wind	$0.45 \cdot (-0.21\ \mathrm{kN/m^2} \cdot 6\ \mathrm{m})$	-

Table 3.7: Load combinations for a span of 6 m.

The combination show the following result.

Dominant load	Permanent load	Leading variable	Accompanying variable	Accompanying variable 2
Snow [kN/m]	3.96	6.48	1.32	-0.567
Wind [kN/m]	3.96	4.41	-0.567	-

Table 3.8: The load combination of a 6 m span.

In order to see which load combination is worst for the frame, the loads have been entered to the software *Robot Structural Analysis* and checked for the forces at the supports and the moments in the corners of the frame. The results are given in Table 3.9 with a figure showing the the local forces on each element, see Figre 3.2. In addition, the reference of nodes from the supports and corners of the frame are illustrated in Figure 3.3.

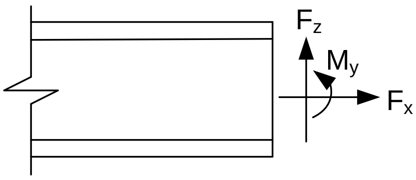

Figure 3.2: Principle sketch of the local forces and moment on a member.

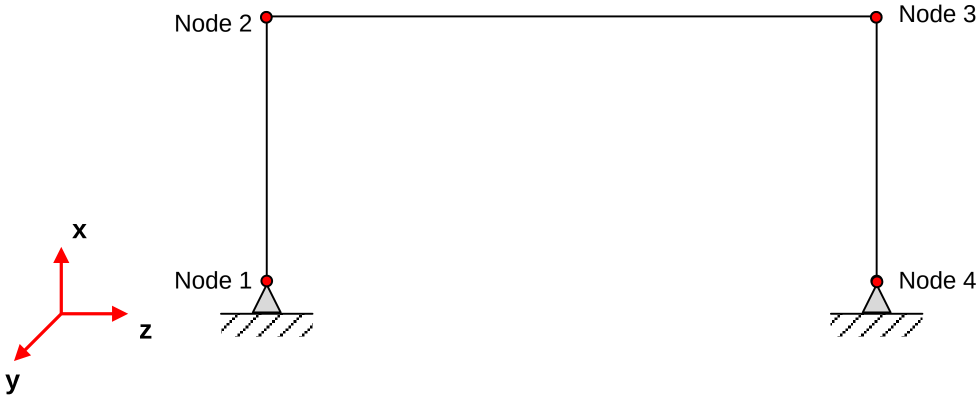

Figure 3.3: Principle sketch of the nodes on the frame.

Node and combination	F_x [kN]	F_z [kN]	M_y [kNm]
Node 1, snow dom.	53.96	123.02	0
Node 4, snow dom.	-63.4	125.38	0
Node 3, snow dom.	-	-	309.89
Node 1, wind dom.	5.52	76.79	0
Node 4, wind dom.	-30.41	83.01	0
Node 3, wind dom.	-	-	144.95

Table 3.9: Results of forces and moment from Robot for different load combinations.

From this it can be seen that when the snow is dominant, the frame will be exposed to the highest loads. Therefore the load combination where snow is dominant will be the basis of the load calculations in this project. This is illustrated in Figure 3.4.

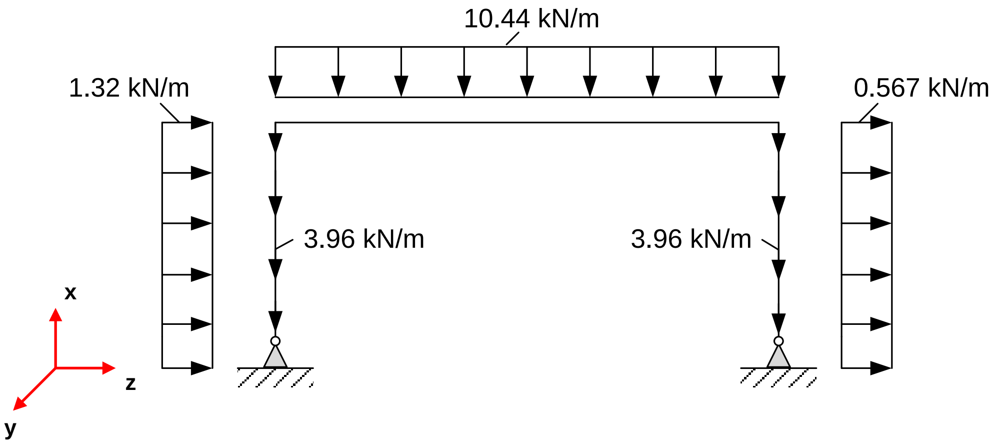

Figure 3.4: The total forces on the frame with snow as the dominant load.

4 Analytical Analysis

The following chapter of the project contains the analytical analysis of the reference frame presented in Chapter 2. The analytical analysis conducted is by the Interaction Formulae found in Eurocode 3 [European Standard, 2005a] where the method takes uniform members in bending and axial compression into account. The method is used to see if a member can resist the bending and axial compression it is subjected to. In this chapter, a description of important parameters and assumptions are stated, in addition to the limitations of Method 1. In the end, the results for the Interaction Formulae for the reference frame is given.

4.1 Eurocode - Method 1

In European Standard [2005a], the following expressions must be satisfied for a member which is subjected to combined bending and axial compression, see Eq.4.1 and 4.2.

$$\frac{N_{Ed}}{\frac{\chi_y N_{Rk}}{\gamma_{M1}}} + k_{yy}\frac{M_{y,Ed}+\Delta M_{y,Ed}}{\chi_{LT}\frac{M_{y,Rk}}{\gamma_{M1}}} + k_{yz}\frac{M_{z,Ed}+\Delta M_{z,Ed}}{\frac{M_{z,Rk}}{\gamma_{M1}}} \leq 1 \tag{4.1}$$

$$\frac{N_{Ed}}{\frac{\chi_z N_{Rk}}{\gamma_{M1}}} + k_{zy}\frac{M_{y,Ed}+\Delta M_{y,Ed}}{\chi_{LT}\frac{M_{y,Rk}}{\gamma_{M1}}} + k_{zz}\frac{M_{z,Ed}+\Delta M_{z,Ed}}{\frac{M_{z,Rk}}{\gamma_{M1}}} \leq 1 \tag{4.2}$$

N_{Ed} , $M_{y,Ed}$, $M_{z,Ed}$	Design values of the compression force and the maximum moments about the *y-y* and *z-z* axis along the member, respectively	[-]
$\Delta M_{y,Ed}$, $\Delta M_{z,Ed}$	Moments due to the shift of the centroidal axis for class 4 sections	[-]
χ_y , χ_z	Reduction factors due to flexural buckling	[-]
χ_{LT}	Reduction factor due to lateral torsional buckling	[-]
k_{yy} , k_{yz} , k_{zy} , k_{zz}	Interaction factors	[-]

In addition, Table 6.7 in Eurocode 3 part 1-1 explains the following values as seen i Eq. (4.3) and (4.3).

$$N_{Rk} = f_y\, A_i \tag{4.3}$$

$$M_{i,Rk} = f_y\, W_i \tag{4.4}$$

f_y	Yield strength	$\left[\text{N/mm}^2\right]$
A_i	Area	$\left[\text{mm}^2\right]$
W_i	Section modulus	$\left[\text{mm}^3\right]$

This means that the following equations can be written, see Eq. (4.5) and (4.6).

$$\frac{N_{Ed}}{\frac{\chi_y f_y A_i}{\gamma_{M1}}} + k_{yy}\frac{M_{y,Ed}+\Delta M_{y,Ed}}{\chi_{LT}\frac{f_y W_i}{\gamma_{M1}}} + k_{yz}\frac{M_{z,Ed}+\Delta M_{z,Ed}}{\frac{f_y W_i}{\gamma_{M1}}} \leq 1 \tag{4.5}$$

$$\frac{N_{Ed}}{\frac{\chi_z f_y A_i}{\gamma_{M1}}} + k_{zy}\frac{M_{y,Ed}+\Delta M_{y,Ed}}{\chi_{LT}\frac{f_y W_i}{\gamma_{M1}}} + k_{zz}\frac{M_{z,Ed}+\Delta M_{z,Ed}}{\frac{f_y W_i}{\gamma_{M1}}} \leq 1 \tag{4.6}$$

4.1.1 Important Parameters and Assumptions

In this section, a short introduction to the major parameters of Eq. (4.5) and (4.6) are presented. There are also examples given on how different parameters change due to different assumptions, showing how Eq. (4.5) and (4.6) may be influenced due to different assumptions.

The references made to this section are from Eurocode 3 European Standard [2005a].

Reduction Factor for Relevant Buckling Mode, χ:

The reduction factor for the relevant buckling curve, χ, is calculated for both *y*- and *z*-axis by the equation seen in Eq. (4.7).

$$\chi = \frac{1}{\Phi + \sqrt{\Phi^2 - \overline{\lambda}^2}} \quad , \quad \chi \leq 1 \tag{4.7}$$

Φ is used to determine the reduction factor. It is calculated as seen in Eq. (4.8).

$$\Phi = 0.5 \left(1 + \alpha \left(\overline{\lambda} - 0.2\right) + \overline{\lambda}^2\right) \tag{4.8}$$

The non-dimensional slenderness, $\overline{\lambda}$ is calculated as follows the following equation, see (4.9).

$$\overline{\lambda} = \sqrt{\frac{A\, f_y}{N_{cr}}} \tag{4.9}$$

N_{cr}	Elastic critical force	[N]

The critical parameter when determining either χ_y or χ_z is N_{cr}. N_{cr} is calculated as seen in Eq. (4.10).

$$N_{cr} = \frac{\pi^2\, E\, I}{l_s^2} \tag{4.10}$$

E	Young's Modulus	$\left[\text{N/mm}^2\right]$
I	Moment of Inertia	$\left[\text{mm}^4\right]$
l_s	Effective length	[mm]

In Eq. (4.10), l_s is the effective length of the buckling length of a member. The effective length is calculated from the original length of the member multiplied by an effective length factor, *K*. The factors are depending on the different support conditions. An illustration of this can be seen in Figure 4.1.

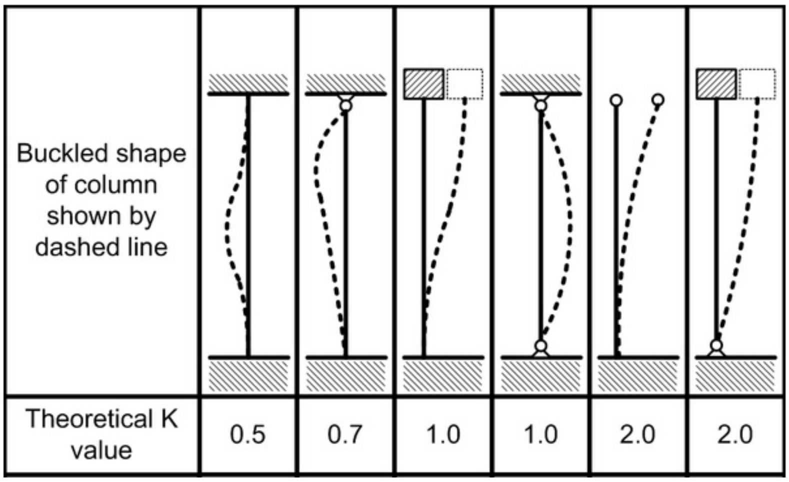

Figure 4.1: Effective length factors [Wikipedia].

In order to see how χ will change by using a different effective length factor, an example has been made where χ_y and χ_z is calculated for the reference frame for both element 2 and 3. The results can be seen in Table 4.1.

Effective length, l_s	Element 2 χ_y [-]	Element 2 χ_z [-]	Element 3 χ_y [-]	Element 3 χ_z [-]
$2.0 \cdot L$	0.0918	0.030	0.735	0.356
$1.0 \cdot L$	0.320	0.110	0.930	0.730
$0.5 \cdot L$	0.735	0.356	1.0	0.926

Table 4.1: Different χ depending on the effective length of the members of the reference frame.

As it can be seen in Table 4.1, χ is depending on the effective length, l_s. Therefore, it is important when designing for a frame, that the assumptions of the effective length are as close to the reality as possible. If not, then as seen in Table 4.1, the reduction factor, χ, may have great impact when Eq. (4.5) and (4.6) is calculated i the end.

The imperfection factor α is also used to determine χ, where α depends on the relationship of h/b and if the section is welded or rolled. However, for the calculation of χ for the reference frame, there is no difference between α as long as the thickness of the flange, t_f, is below 40 mm ($t_f \geq 40$ mm). This means that for this project the α factor is constant.

Reduction Factor for Lateral Torsional Buckling Curves, χ_{LT}:

There are two different ways of determining χ_{LT}. There is a general method and a second method that is applicable for rolled or equivalent welded sections. From European Standard [2005a], it can be seen from the equations used to calculate χ_{LT}, that choosing the first general method will give a lower value than the second method of rolled or equivalent sections. However, as the reference frame consists of a rolled or equivalent section, the second method is used for the calculation.

When choosing the second method, European Standard [2005a] states that χ_{LT} may be modified. The modification value, f, can be found in the Danish National Annex where it is stated that $f = 1$ as the moment distribution is included in the determination of M_{cr}. This means that in this case, χ_{LT} is not modified.

The reduction factor for lateral-torsional buckling, χ_{LT}, is determined as the following, see Eq. (4.11).

$$\chi_{LT} = \frac{1}{\Phi_{LT} + \sqrt{\Phi_{LT}^2 - \beta\,\overline{\lambda}_{LT}^2}} \tag{4.11}$$

Φ_{LT}	Factor used to calculate χ_{LT}	[-]
$\overline{\lambda}_{LT}$	Non-dimensional slenderness	[-]

According to European Standard [2005a], the following values are recommended for rolled or equivalent sections:

$$\overline{\lambda}_{LT,0} = 0.4 \quad \text{(Maximum value)}$$
$$\beta = 0.75 \quad \text{(Minimum value)}$$

Φ_{LT} is calculated in order to determine χ_{LT}. This is done by the following, see Eq. (4.12)

$$\Phi_{LT} = 0.5\,\left(1 + \alpha_{LT}\,\left(\overline{\lambda}_{LT} - \overline{\lambda}_{LT,0}\right) + \beta\,\overline{\lambda}_{LT}^2\right) \tag{4.12}$$

The non-dimensional slenderness $\overline{\lambda}_{LT}$ is calculated as seen in Eq. (4.13).

$$\overline{\lambda}_{LT} = \sqrt{\frac{W_{pl,y}\,f_y}{M_{cr}}} \tag{4.13}$$

The critical parameter when calculating χ_{LT} is M_{cr}, where M_{cr} is the elastic critical moment for lateral torsional buckling found in Eq. (4.13). M_{cr} is calculated as the following, see (4.14).

$$M_{cr} = m_n\,\frac{E\,I_z}{l^2}\,h_t \tag{4.14}$$

m_n	Value given by table from Mohr and et al. [2009] for the case investigated	[-]
h_t	Height of C-S from the middle of top flange to middle of bottom flange	[mm]

For the calculation of the reduction factor for lateral torsional buckling, χ_{LT}, it is important to find and use the correct value for m_n and to determine if the elements are constrained or unconstrained when it comes to lateral torsional buckling.

Non-dimensional Slenderness for Lateral Torsional Buckling, $\overline{\lambda}_{LT}$:

The non-dimensional slenderness is a part of the calculation where the formula takes the slenderness of a member into account. The slenderness of a member is important for a frame where a member may buckle before it yields.

Interaction factors, k_{ij}:

The interaction factors are for combined axial compression and bending. In order to calculate the interaction factors, a decision between two different alternative approaches must be done. In Note 2 in Section 6.3.3 from European Standard [2005a], it is stated that the National Annex may give a choice in which of the alternatives should be used. In the Danish National Annex, it is stated that one can freely choose between the methods. The recommendations however are as follows:

“Method 1 is recommended for significant structures, when economy is crucial and by preparation of a calculation software” [European Standard, 2005a].

“Method 2 is recommended as a more simplifying method at less significant structures”[European Standard, 2005a].

Even though economy plays an important role when constructing a frame, this project does not prepare for a calculation program. In addition, the frame is not a significant structure. This means that for this project, the second more simplifying method is chosen for the calculation of the interaction factors.

An important decision to make when determining the interaction factors is choosing the right moment distribution diagram to follow. The European Standard [2005a] gives a standard moment distribution diagram for method 2 that can be seen in Figure 4.2.

Moment diagram	range		C_{my} and C_{mz} and C_{mLT} uniform loading	C_{my} and C_{mz} and C_{mLT} concentrated load
	$-1 \leq \psi \leq 1$		$0,6 + 0,4\psi \geq 0,4$	
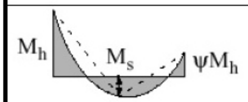 $\alpha_s = M_s/M_h$	$0 \leq \alpha_s \leq 1$	$-1 \leq \psi \leq 1$	$0,2 + 0,8\alpha_s \geq 0,4$	$0,2 + 0,8\alpha_s \geq 0,4$
	$-1 \leq \alpha_s < 0$	$0 \leq \psi \leq 1$	$0,1 - 0,8\alpha_s \geq 0,4$	$-0,8\alpha_s \geq 0,4$
		$-1 \leq \psi < 0$	$0,1(1-\psi) - 0,8\alpha_s \geq 0,4$	$0,2(-\psi) - 0,8\alpha_s \geq 0,4$
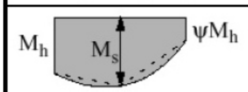 $\alpha_h = M_h/M_s$	$0 \leq \alpha_h \leq 1$	$-1 \leq \psi \leq 1$	$0,95 + 0,05\alpha_h$	$0,90 + 0,10\alpha_h$
	$-1 \leq \alpha_h < 0$	$0 \leq \psi \leq 1$	$0,95 + 0,05\alpha_h$	$0,90 + 0,10\alpha_h$
		$-1 \leq \psi < 0$	$0,95 + 0,05\alpha_h(1+2\psi)$	$0,90 - 0,10\alpha_h(1+2\psi)$

Figure 4.2: Equivalent uniform moment factors C_m [European Standard, 2005a].

The factor C_{my} is included in the calculation of the interaction factor k_{ij}. In order to illustrate how it is possible to determine different moment diagrams for the same element, an example is given of element 3. Element 3 has originally a moment diagram distribution of a triangle, where at the bottom of the support, the moment equals zero, see Figure 4.3. However, if the effective length used to determine χ is taken into account, the moment distribution changes. This means that if an effective length of two times the original length is used, C_{my} and in the end k_{yy} and k_{zy} will change. This is illustrated in Figure 4.3.

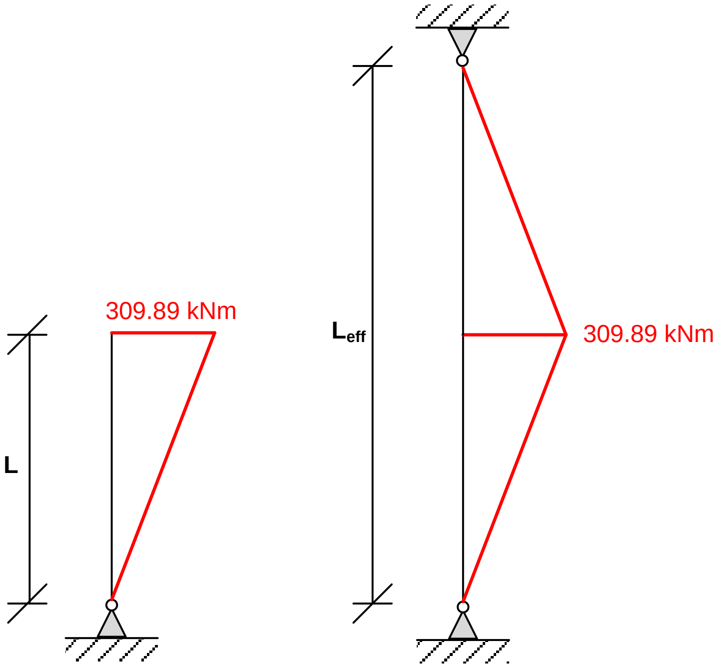

Figure 4.3: Different moment distributions according to original length and effective length of element (3)
.

The different C_{my}, k_{yy} and k_{zy} based on the different moment distributions are compared to each other in Table 4.2.

Moment distribution from	C_{my} [-]	k_{yy} [-]	k_{zy} [-]
Original length	0.6	0.984	0.590
Effective length	0.95	0.623	0.373

Table 4.2: k_{yy} and k_{zy} calculated for different moment distributions on element (3) .

From Table 4.2, it can be seen that there is a significant difference in the k_{yy} and k_{zy} factors depending on the moment distribution chosen. The question then becomes if the moment distribution should be according to the effective length of the member or to the original length of the member.

It should also be stated that k_{zz} and k_{yz} equals zero as there is no moment about the z-axis.

4.2 Limitations of Interaction Formulae

In order to use the equations given for the Interaction Formula, which takes uniform members in bending and axial compression into account, it is required, according to Eurocode 3 [European Standard, 2005a], that the member consists of a profile with constant cross-section. If a member varies in the cross-section, the General Method, should be used. How the General Method is applied can be seen in Chapter 5.

4.3 Calculation of a Frame Profile

All of the calculations of the frame has been calculated in MATLAB-codes. The codes can be seen in the Digital Appendix, see A.11 and A.12.

Interaction Formulae is used to calculate a profile that is suited for the reference frame. In order to find a suited profile, a MATLAB code has been made. The program is calculating the utilization ratio for the Interaction Formulae by using Equation (4.1) and (4.2). The input parameters of the program are the section properties, the compression force and moment, and different assumptions such as the effective length of buckling and of lateral torsional buckling and C_{my}. Different profiles have been investigated to find a profile with the utilization ratio closes to 1.0 (100%). In Appendix B, a worked example of a HE320A profile has been done. The calculation is an elaboration on how method 1 is implemented.

The MATLAB code has been used for the investigation of HE320A. The profile will be used for the reference frame so that the utilization ratio for Method 1 and the General Method can be compared.

4.3.1 Results of HE320A for Element 3

In this section, a summary of the results from the Interaction Formulae calculation will be given, in addition to what was found critical during the calculation for element 3. The calculation and assumptions for the results can be seen in Appendix B. It should also be noted that element 3 is chosen instead of element 1 as this element has a higher compression force and bending moment.

The results from Interaction Formulae can be seen in Table 4.3.

Description	Symbol	Value	Unit
Greatest compression force	N_{Ed}	125.38	[kN]
Greatest moment	M_{Ed}	309.89	[kNm]
Critical compression force *y* axis	N_{cr}	1744.1	[kN]
Critical compression force *z* axis	N_{cr}	5786.7	[kN]
Critical moment	M_{cr}	2925.1	[kNm]
Reduction factor for relevant buckling mode	χ_{y}	0.447	[-]
Reduction factor for relevant buckling mode	χ_{z}	0.73	[-]
Reduction factor for lateral torsional buckling	χ_{LT}	1.0	[-]
Interaction factor	k_{yy}	0.984	[-]
Interaction factor	k_{yz}	0.0	[-]
Interaction factor	k_{zy}	0.59	[-]
Interaction factor	k_{zz}	0.0	[-]
Utilization of Equation (4.1)		1.09	[-]
Utilization of Equation (4.2)		0.66	[-]

Table 4.3: The results for Interaction Formulae for element 3 of HE320A.

From Table 4.3, it can be seen that the utilization ratio about the *y* axis is 1.09 (109 %).

The results from the calculations, see Appendix B, shows that buckling effects may not be ignored for this section due to the slenderness of the element. In addition, it is so that lateral torsional buckling effects may be ignored and only cross-sectional checks will apply.

4.3.2 Results of HE320A for Element 2

In this section, the results from the Interaction Formulae calculation will be given in addition to what was found critical during the calculation for element 2. The calculation and assumptions for the results can be seen in Appendix B.

The results from Interaction Formulae can be seen in Table 4.4.

Description	Symbol	Value	Unit
Greatest compression force	N_{Ed}	60.56	[kN]
Greatest moment	M_{Ed}	309.89	[kNm]
Critical compression force y axis	N_{cr}	840.31	[kN]
Critical compression force z axis	N_{cr}	361.67	[kN]
Critical moment	M_{cr}	3072.1	[kNm]
Reduction factor for relevant buckling mode	χ_{y}	0.249	[-]
Reduction factor for relevant buckling mode	χ_{z}	0.11	[-]
Reduction factor for lateral torsional buckling	χ_{LT}	1.0	[-]
Interaction factor	k_{yy}	0.791	[-]
Interaction factor	k_{yz}	0.0	[-]
Interaction factor	k_{zy}	0.475	[-]
Interaction factor	k_{zz}	0.0	[-]
Utilization of Equation (4.1)		0.87	[-]
Utilization of Equation (4.2)		0.70	[-]

Table 4.4: The results for Interaction Formulae for element 2 of HE320A.

From Table 4.4, it can be seen that the utilization ratio about the y axis is the highest at 0.87 (87 %).

The results from the calculations, see Appendix B, shows that buckling effects may not be ignored for this section due to the slenderness and the compression force of the element. In addition, it is so that lateral torsional buckling effects may be ignored and only cross-sectional checks will apply.

4.4 Summary

This section will display a summary of the utilization ratio for both element 2 and 3, see Table 4.5.

Element	y axis	z axis
Element 2	0.87	0.70
Element 3	1.09	0.66

Table 4.5: Summary of utilization ratio for element 2 and 3 of HE320A for Interaction Formulae.

From 4.5, it can be seen that the worst element of the frame is element 3 as this element has a utilization ratio above 100%. The utilization ratio about the z axis is also higher for element 3 than element 2.

5 General Method

The following chapter contains an investigation of the reference frame presented in Chapter 2 by the General Method [European Standard, 2005a]. The General Method allows to make use of a *Finite Element Analysis* (FEA) to determine the two load amplifiers, $\alpha_{\text{ult,k}}$ and $\alpha_{\text{cr,op}}$, cf. Section 5.1. Therefore, the engineering simulation program *Abaqus/CAE* is used to perform the analysis because it makes use of the *Finite Element Method* (FEM). Brief descriptions of the background for the *Finite Element Method* (FEM) and *Abaqus/CAE* are given in Appendix C and D, respectively.

5.1 General Method

The General Method is a method described in Section 6.3.4 in European Standard [2005a] to investigate if lateral and lateral torsional buckling of structural components occur, and it takes into account the out-of-plane stability of a frame by a global reduction factor, χ_{op}. The method can be used where the method explained in Chapter 4 does not apply e.g. when the C-S of the steel profile used is varying in dimensions. Eq. (5.1) shows the condition which has to be fulfilled for the frame to resist out-of-plane buckling for any of the structural components.

$$\frac{\chi_{\text{op}}\ \alpha_{\text{ult,k}}}{\gamma_{\text{M1}}} \geq 1.0 \tag{5.1}$$

$\alpha_{\text{ult,k}}$	Minimum load amplifier of the design loads to reach the characteristic resistance of the most critical cross-section of the structural component considering its in-plane behaviour without taking lateral or lateral torsional buckling into account however accounting for all effects due to in-plane geometrical deformation and imperfections, global and local, where relevant	[-]
χ_{op}	Global reduction factor for the non-dimensional slenderness $\overline{\lambda}_{\text{op}}$	[-]
γ_{M1}	Partial factor for resistance of members to instability assessed by member checks, $\gamma_{\text{M1}} = 1.20$	[-]

One of the difficult parameters to determine by a hand calculation is the mininum load amplifier, $\alpha_{\text{ult,k}}$. This minimum load amplifier can be determined by a non-linear analysis of a frame modelled by two-dimensional beam elements on which the loads are increasing incrementally. Even though the model is two-dimensional, the analysis remains geometrically and materially non-linear, and in-plane bow and sway imperfections are taken into account by the analysis where relevant, but out-of-plane sway imperfections are not included. Appendix E describes how to take these imperfections into account.

The global reduction factor for out-of-plane buckling, χ_{op}, is determined by another parameter which is also difficult to determine by a hand calculation. That parameter is the minimum load amplifier, $\alpha_{\text{cr,op}}$, for the in-plane design loads to reach the elastic critical resistance of the structural component with regards to lateral or lateral torsional buckling without accounting for in-plane flexural buckling, which can be evaluated by modelling the frame with three-dimensional shell elements.

The General Method is advantageous compared to the method used in Chapter 4 since it is able to take into account e.g. varying C-S of the members of the frame. It is a numerical method and

Finite Element (FE) software may be used to determine the two load amplifiers contained in Eq. (5.1).

As described in Appendix C, the *Finite Element Method* (FEM) contains three steps - a *Preprocessing*, *Simulation* and *Postprocessing* step. These steps and the contents of them according to the numerical analysis performed on the reference frame are described in the following sections. The results of the analysis and the determination of the two load amplifiers are shown in the *Postprocessing* step in Section 5.4.

5.2 Preprocessing

In the *Preprocessing* step, the reference frame is modelled in *Abaqus/CAE* as described in Chapter 2 where the statical model and thereby also the boundary conditions of the frame are set up. The geometry of the frame is shown in Figure 2.2, and the material properties are given in Table 2.1. The most critical load scenario for the frame is found in Chapter 3.

5.2.1 Finite Element Types

It is of great importance when analysing a finite element model to apply the appropriate type of element to the model being analysed. *Abaqus/CAE* has access to a database containing a large number of different element types categorized based on family, degrees of freedom, number of nodes, order of interpolation, formulation and integration.

The given reference frame is modelled by two different types of finite elements - beam elements and shell elements shown to the left and to the right in Figure 5.1, respectively. The difference between beam and shell elements is that the beam elements are one-dimensional and are used for modelling structures in which one dimension (the length) is significantly greater than the other two dimensions and in which the longitudinal stress is most important. In contrast to beam elements, shell elements are two-dimensional and are used for modelling structures in which one dimension (the thickness) is significantly smaller than the other two dimensions and in which the stresses in the thickness direction are negligible.

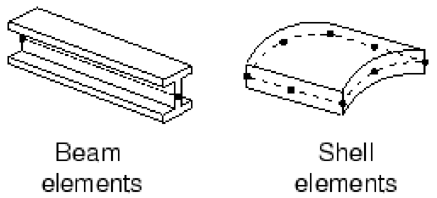

Figure 5.1: Beam elements and shell elements [SIMULIA, 2012].

The choice of finite element type and the number of finite elements influence the level of detail of the model. The level of detail of the model increases by using shell elements compared to beam elements because the number of finite elements increases. However, the computation time is also increasing when using shell elements instead of beam elements.

5.2.2 Modelling by Beam Elements

Firstly, the reference frame is modelled by the simpler beam elements to give a preliminary estimate of the behaviour of the frame due to instability and to determine the minimum load amplifier, $\alpha_{ult,k}$, cf. Section 5.1. The C-S of the applied steel profile has to be defined when using beam elements to model the frame. This is done by defining a generalised beam profile using C-S engineering properties - in this case of an I-beam. The C-S properties of a HE320A profile, which is the beam profile used, are shown in Table B.2. In *Abaqus/CAE*, beam elements are modelled as lines. Therefore, the figures in the following sections are illustrated with a graphical option switch on to show the C-S of the steel profile used to model the reference frame. The units used in *Abaqus/CAE* for the beam element model are millimetres [mm] for the dimensions, megapascals [MPa] for the modulus of elasticity, E, and thus newtons per millimetre [N/mm] for the loads. This can be seen in Figure 5.2. The beam element model made in *Abaqus/CAE* can be found in Digital Appendix A.1.

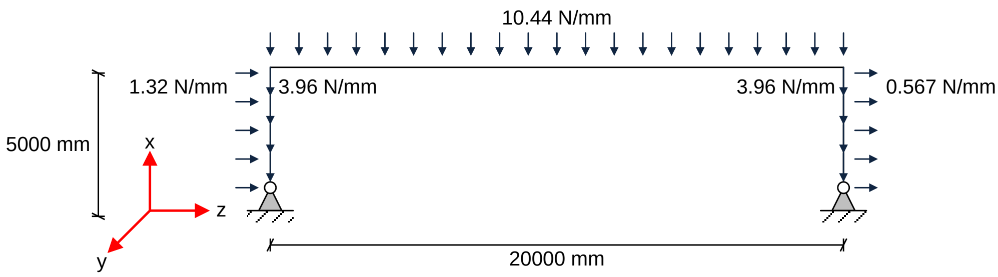

Figure 5.2: Units used in the beam element model in *Abaqus/CAE*.

Mesh

The beam element model is constructed of 2-noded linear beam elements in space. The meshed beam element model is shown in Figure 5.3.

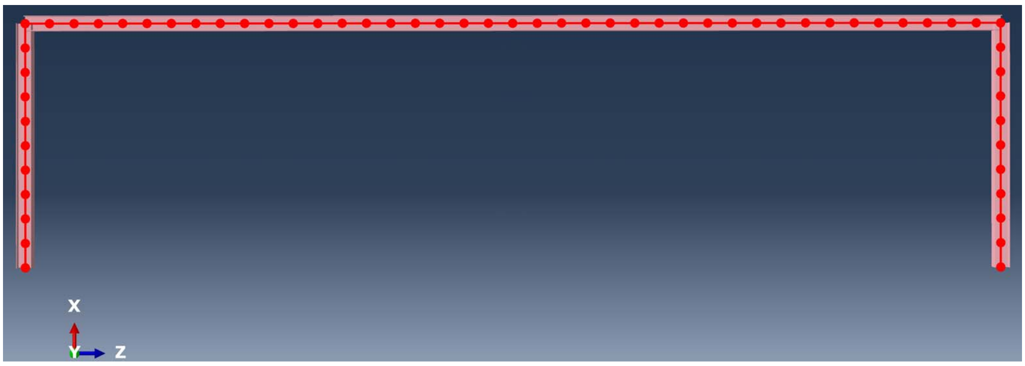

Figure 5.3: Mesh of the beam element model shown in 2D.

The discretization of the beam element model is set to 500, and this results in an element size in the length scale of 500 mm. A beam element cut out from element 2 of the frame is shown in Figure 5.4. The black dots in the figure are the two nodes representing the beam element.

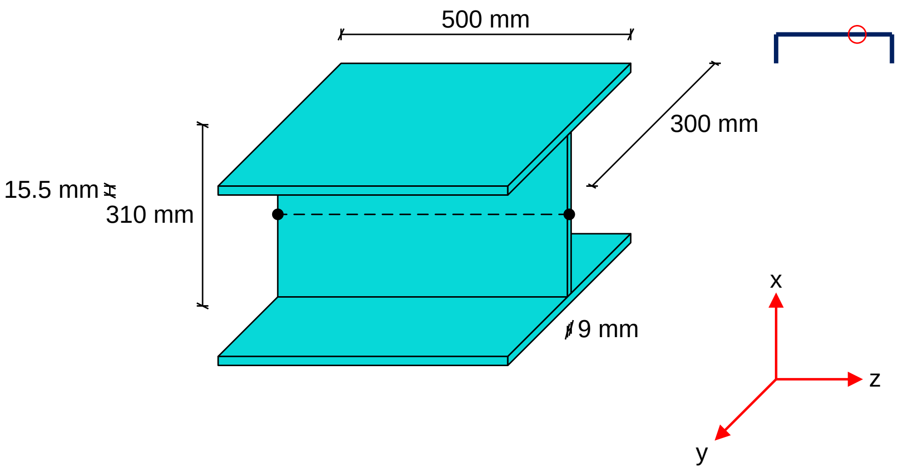

Figure 5.4: Beam element cut out from element (2) of the frame.

Boundary Conditions

In *Abaqus/CAE*, the pinned support conditions of the frame are established by fixing the displacement in both directions $(U_x = U_z = 0)$ and thereby establishing a charnier and letting the frame rotate freely around the y axis. This is shown in Figure 5.5.

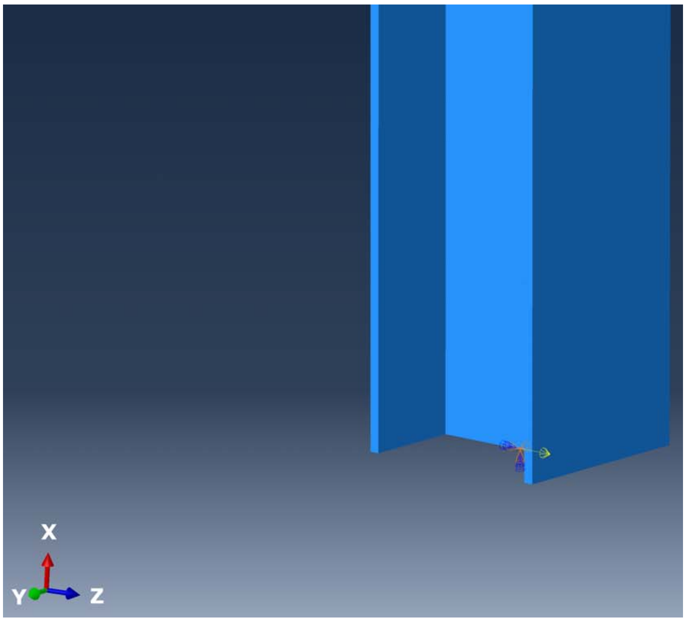

Figure 5.5: Pinned support condition in the beam element model shown in 3D.

Loads

Since the model is constructed as a two-dimensional model, the loads can only be applied by uniformly distributed line loads. As described in Chapter 3, element (1) and (3) are affected by pressure and suction, respectively, coming from the wind load. Figure 5.6 shows the loading applied to the reference frame modelled by beam elements.

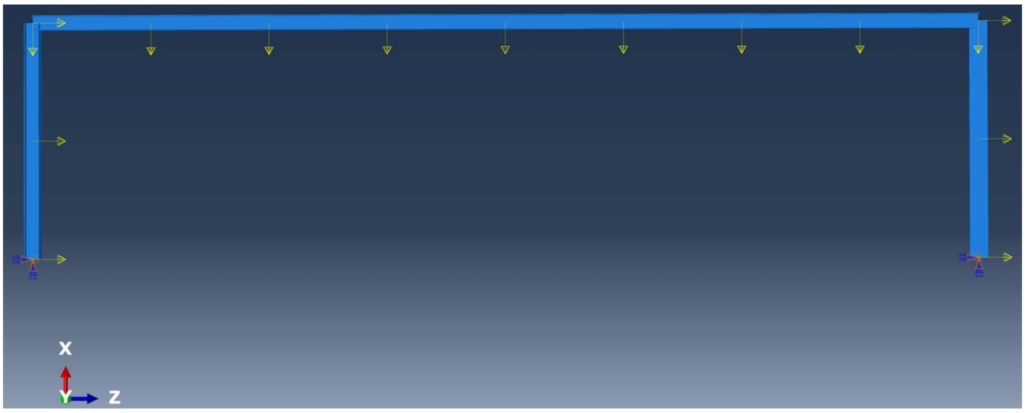

Figure 5.6: Uniformly distributed line load applied to the reference frame modelled by beam elements shown in 2D.

5.2.3 Modelling by Shell Elements

To do a more detailed analysis of the behaviour of the reference frame due to instability and to determine the other minimum load amplifier, $\alpha_{cr,op}$, the frame is modelled by the more advanced shell elements. The modelling of the frame by shell elements is done separately meaning that the two flanges and the web are modelled individually by parts and afterwards merged together. The units used in *Abaqus/CAE* for the shell element model are millimetres [mm] for the dimensions, megapascals [MPa] for the modulus of elasticity, E, and thus newton per square millimetres [N/mm^2] for the pressures applied as the loads. This can be seen in Figure 5.7. The self-weight of the reference frame is inflicted by specifying the density of steel, ρ, and applying gravity ($g = 9.81$ N/kg) to it as well. The shell element model made in *Abaqus/CAE* can be found in Digital Appendix A.3.

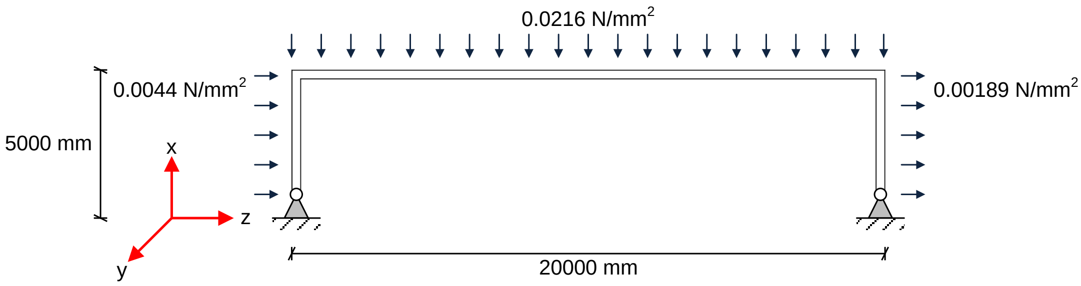

Figure 5.7: Units used in the shell element model in *Abaqus/CAE*.

Mesh

The shell element model is constructed of 4-noded doubly curved shell elements. The meshed shell element model is shown in Figure 5.8.

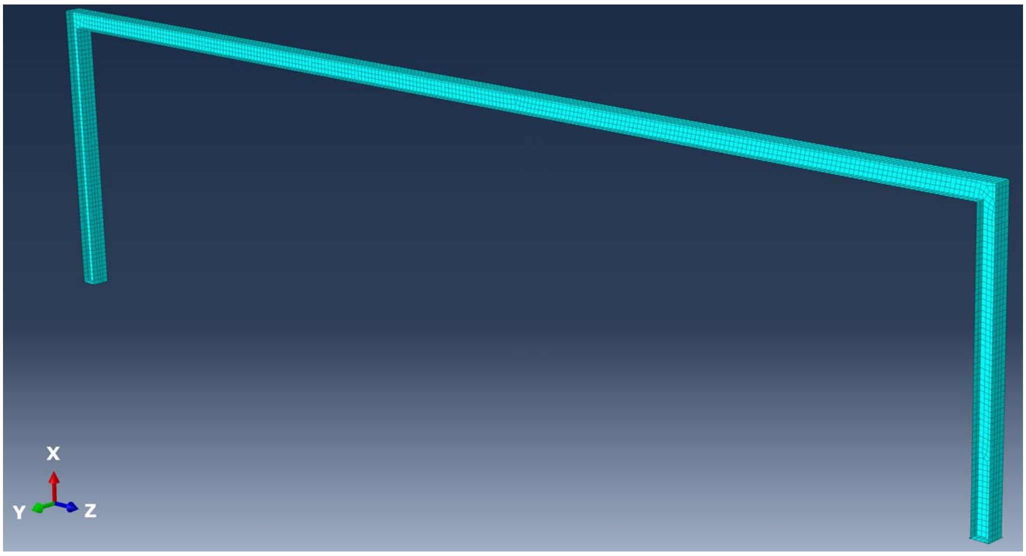

Figure 5.8: Mesh of the shell element model shown in 3D.

The discretization of the shell element model is chosen to be 80 which results in an element length of 80 mm as shown in Figure 5.9. Figure 5.9 also shows the dimensions of the shell elements representing the flanges and the web, respectively, of a cut out of element (2). The black dots on the elements are the four nodes representing the shell element.

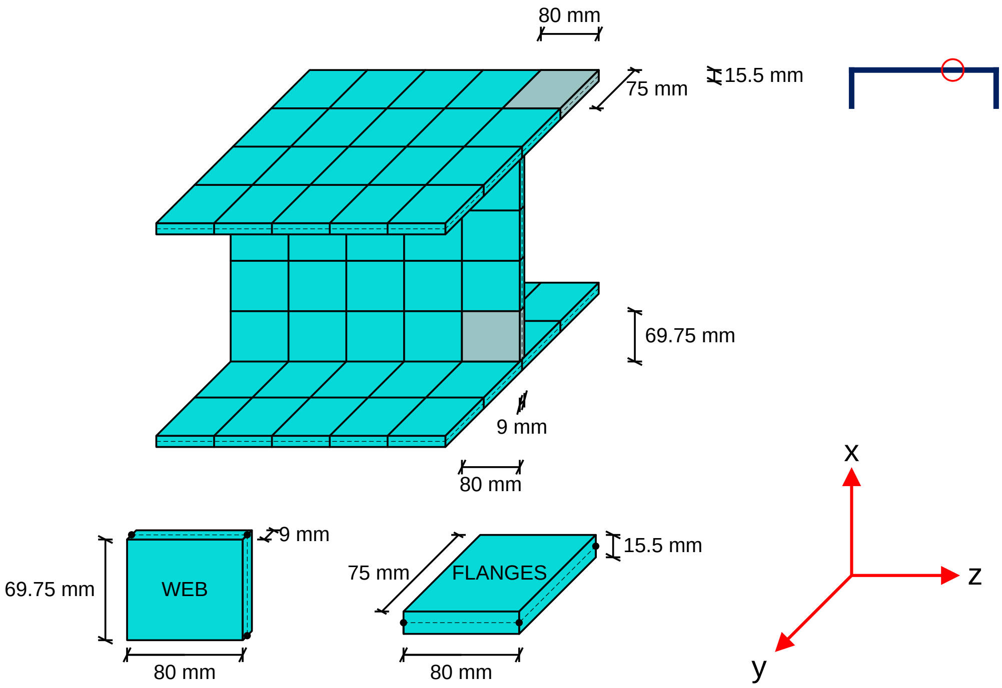

Figure 5.9: Cut out of meshed element (2) with the dimensions of the shell elements. The shell elements are illustrated by the darker areas. A shell element of the web and the flange are, respectively, illustrated in the bottom of the figure.

The mesh is detailed enough for a global analysis of the frame. If an investigation of the corners of the frame was of interest, the mesh should have been refined in these areas or refined all over the frame.

Boundary Conditions

The pinned supports of the reference frame are constructed by using the boundary conditions of the model. The boundary conditions are made by using two plates with a thickness of 20 mm, an area of the C-S dimensions of the HE320A profile, cf. Figure 2.3, plus 10 mm in all directions for weldings and with the same material properties as the reference frame, cf. Section 2.4. These plates are merged to the reference frame at the bottom of element 1 and 3, and the boundary conditions are then established in two points in a distance of 105 mm from the edge of the plate in the centerline of each plate by fixing the displacements in all directions $\left(U_{\mathrm{x}} = U_{\mathrm{y}} = U_{\mathrm{z}} = 0\right)$ and the rotation around the x axis $(U_{\mathrm{Rx}} = 0)$. These boundary conditions are assumed to represent two bolts placed on each side of the profile for the fastening of the frame. Thereby, a chanier is constructed letting the frame freely rotate around the y and z axis at the bottom of element 1 and 3. This principle is shown in both Figure 5.10 and 5.11 where the transparent orange plane is drawn to illustrate that the profile is cutted here.

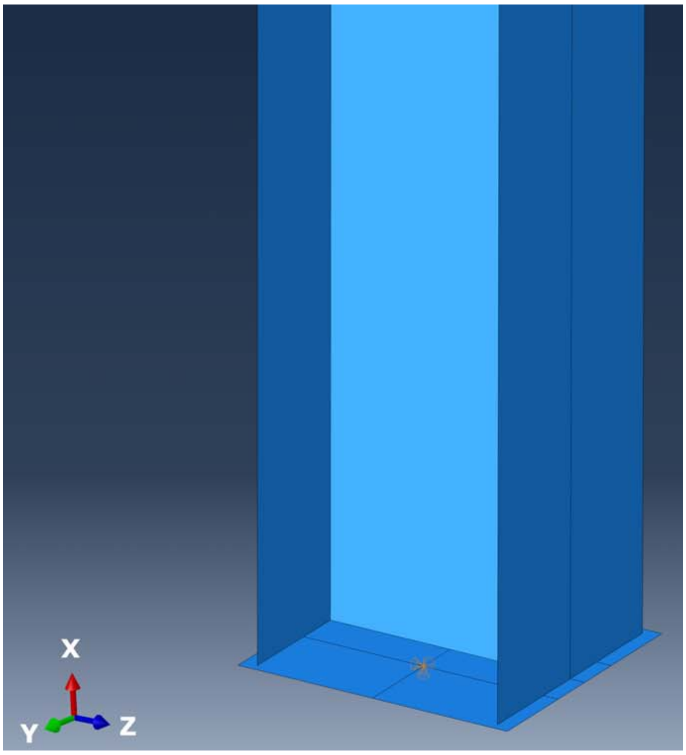

Figure 5.10: Pinned support condition in the shell element model shown in 3D.

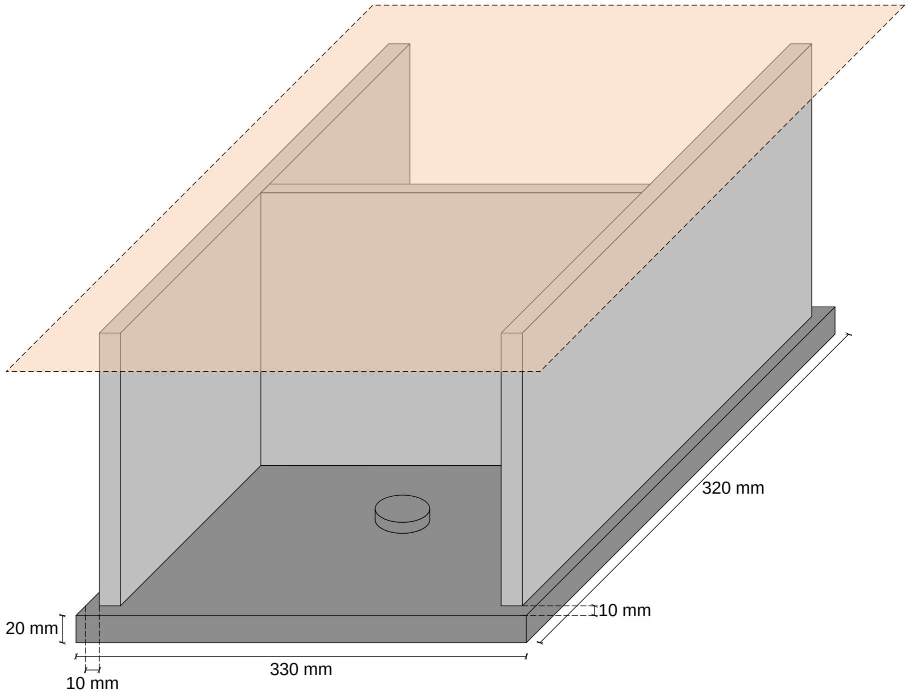

Figure 5.11: Principle sketch of plate used to make the pinned supports. The transparent orange plane is drawn to illustrate that the profile is cutted here.

These pinned supports could also have been modelled as done with the beam elements in Section 5.2.2 or by applying the boundary conditions to all the lines forming the C-S of the profile but this will either lead to infinitely large stresses in the area of the support or an unrealistic representation of a pinned support condition, respectively.

Boundary conditions are also established in the corners of the reference frame at the outer flanges where the supporting conditions are assumed to be as fork supports. Thereby, the reference frame is fixed for out-of-plane displacement $\left(U_{\mathrm{y}} = 0\right)$ and for rotation around the x and z axis $(U_{\mathrm{Rx}} = U_{\mathrm{Rz}} = 0)$.

Loads

The uniformly distributed surface loads are applied to the frame by inflicting a pressure on the outer flanges of the frame as shown in Figure 5.12. Element 1 and 3 are, respectively, subjected to pressure and suction. The suction is modelled by a negative pressure on the outer flange of element 3.

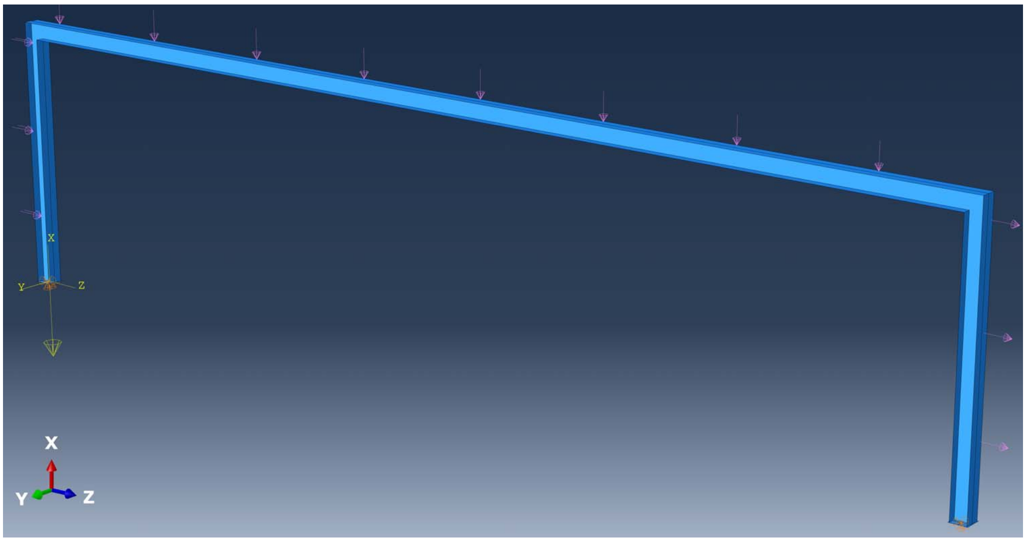

Figure 5.12: Uniformly distributed surface loads applied to the reference frame modelled by shell elements shown in 3D.

5.3 Simulation

The *Simulation* step is the step where the actual numerical analysis is performed. A full analysis is conducted to get the output data which are used in the *Postprocessing* step to make a plot of the displacement in the x direction (u_{x}) against the load exerted, q, and thereby, getting the in-plane minimum load amplifier, $\alpha_{\text{ult,k}}$, by the beam element model. The out-of-plane minimum load amplifer, $\alpha_{\text{cr,op}}$, is determined by solving an eigenvalue problem which gives an eigenvalue related to an out-of-plane buckling mode. The eigenvalue is equal to the out-of-plane minimum load amplifier, $\alpha_{\text{cr,op}}$. An analysis in *Abaqus/CAE* can take from a few seconds to a couple of days to complete depending on the complexity of model being analysed and the power of the computer used for the analysis. The *Simulation* step is similar for both the beam element model and the shell elemnt model. Table 5.1 shows the number of elements and nodes for each of the models.

Element model	Discretization of element model	Number of elements	Number of nodes
Beam element model	500	60	61
Shell element model	80	4465	4829

Table 5.1: Number of elements and nodes for the beam and shell element model, respectively.

As shown in Table 5.1, the shell element model is more detailed because of the larger number of elements and nodes, and it is therefore better modelling and visualizing the effects of instability of the reference frame.

It is chosen to use an increment size of 0.01 and thus the loads are increased 1 % in each step. If the model is not able to withstand the increase in loading, the increment size is halved and in this way, *Abaqus/CAE* continues to apply the loads until the minimum increment size is reached. This minimum incremenet size is chosen to be 10^{-10}.

5.3.1 Convergence Analysis

The level of detail of the mesh is investigated by a convergence analysis for both the beam and the shell element model, respectively. The convergence analysis for the beam element model is shown in Figure 5.13, where it can be seen that the discretization of 500 mm is sufficient for the beam element model to give reasonable results as the curve approximates a certain displacement with an element length of around 500 mm.

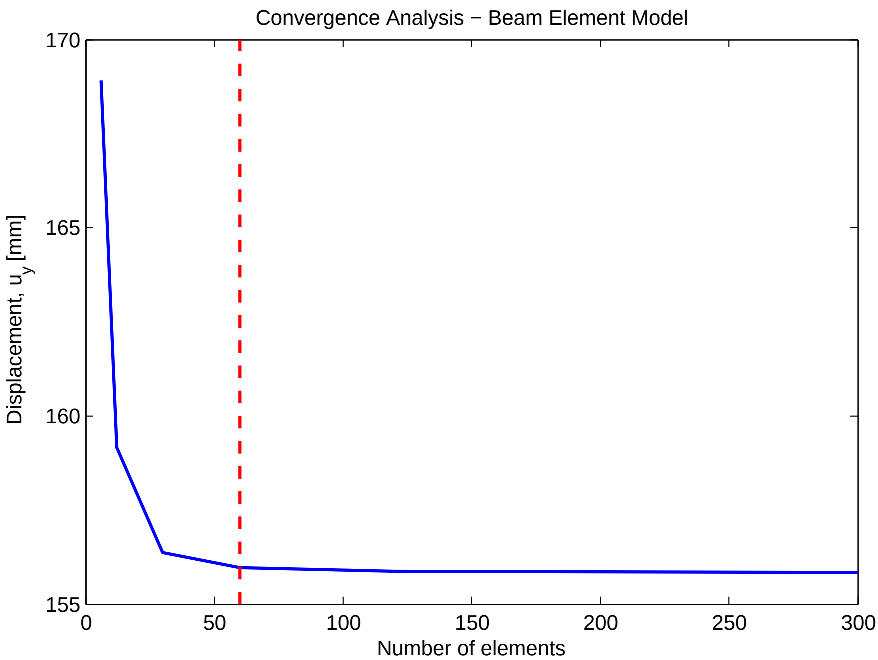

Figure 5.13: Convergence analysis for the beam element model.

Likewise, a convergence analysis is conducted on the shell element model. This is shown in Figure 5.14, whwre it can be seen that a discretization of 80 mm is sufficient for the shell element model as well to give reasonable results.

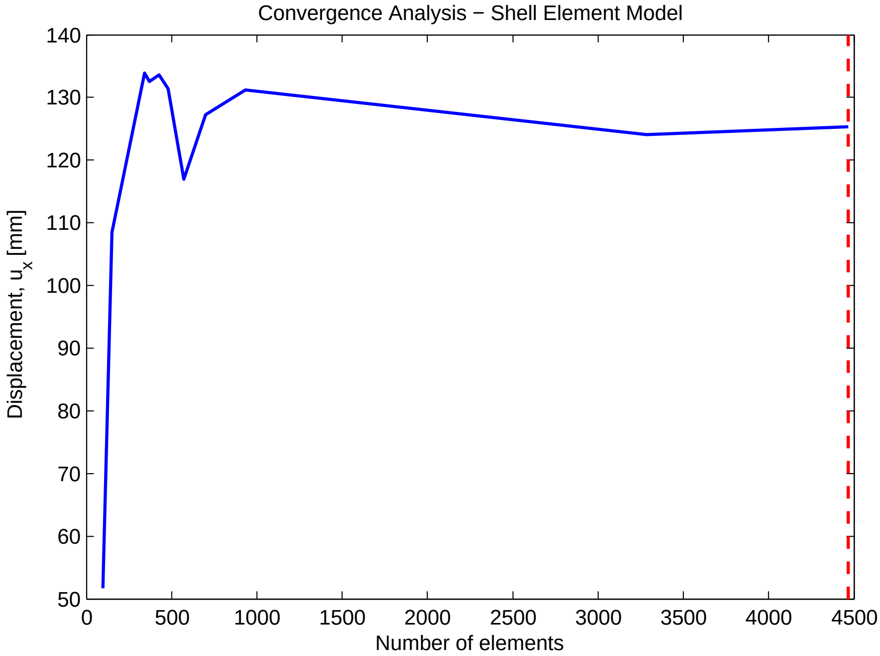

Figure 5.14: Convergence analysis for the shell element model.

5.4 Postprocessing

The following section contains the results of the analyses of the beam and the shell element model, respectively. During this section the two minimum load amplifiers, $\alpha_{\text{ult,k}}$ and $\alpha_{\text{cr,op}}$, will be determined to calculate the utilization ratio, UR, by the General Method, so the two methods can be compared to each other in Chapter 6. The calculations are shown in Appendix G and in Digital Appendix A.9.

5.4.1 Determination of the Minimum Load Amplifier, $\alpha_{\text{ult,k}}$

The minimum load amplifier, $\alpha_{\text{ult,k}}$, is related to the in-plane behaviour of the reference frame. It is determined by plotting the displacement, u_{x}, of element 2 in the x direction against the load exerted, q, as shown in Figure 5.15 for the beam element model.

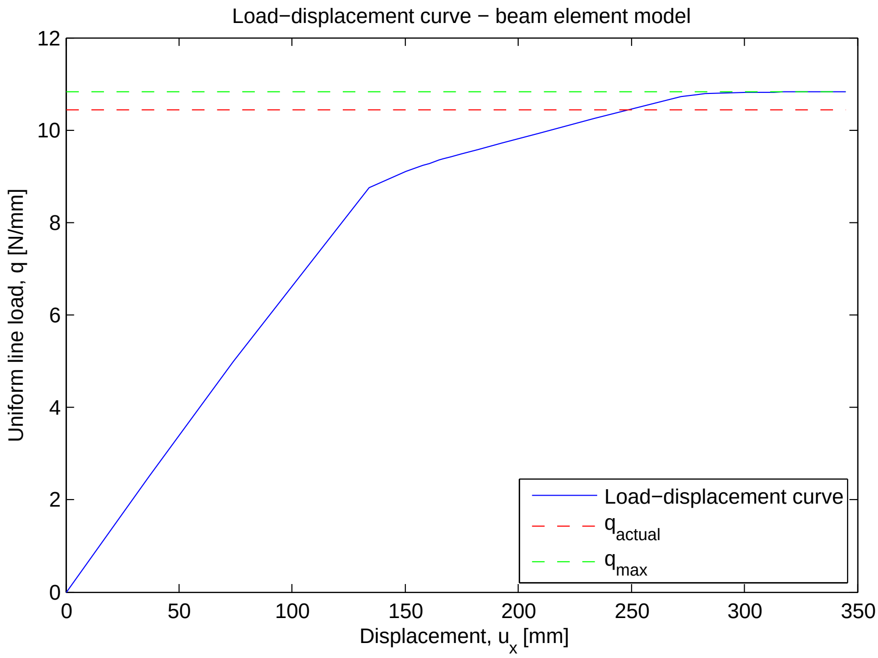

Figure 5.15: Load-displacement curve for the beam element model.

As shown in Figure 5.15, the reference frame is loaded until failure occurs $\left(f_y = 235 \text{ MPa}\right)$, and the load-displacement curve can then be used to approximate the failure load, q_{max}, which is used in the determination of the minimum load amplifier, $\alpha_{\text{ult,k}}$, where the relation between the failure load, q_{max}, and the load actually applied, q_{actual}, results in the minimum load amplifier, $\alpha_{\text{ult,k}}$. This principle is shown in Eq. (5.2).

$$\alpha_{\text{ult,k}} = \frac{q_{\text{max}}}{q_{\text{actual}}} \tag{5.2}$$

q_{max}	Failure load	[N/mm]
q_{actual}	Actual load	[N/mm]

The result of the determination of the minimum load amplifier, $\alpha_{\text{ult,k}}$, for the in-plane behaviour is shown in Table 5.2.

Method	$\alpha_{\text{ult,k}}$ [-]
Beam Element Model	1.0378

Table 5.2: Minimum load amplifier, $\alpha_{\text{ult,k}}$, for in-plane behaviour.

Imperfections

In the determination of $\alpha_{\text{ult,k}}$, the following should be included in the calculation of this factor as stated in European Standard [2005a] "[...] accounting for all effects due to in-plane geometrical deformation and imperfections, global and local, where relevant". This means that only where it is relevant, in-plane geometrical deformation and imperfections must be taken into consideration. In order to investigate if the imperfections are relevant to incorporate in this project, imperfections are implemented on the reference frame, and the results are compared to the results without imperfections on the reference frame. The reference frame modelled by beam elements in *Abaqus/CAE* is given global initial sway imperfections and initial local bow imperfections in coherence with the recommendations from European Standard [2005a], see Appendix E. In Table 5.3, the load multiplier for the maximum load on the reference frame at the yielding limit is shown for the reference frame with and without imperfections.

Imperfections	Load multiplier
None	0.010835
Both sway and initial bow	0.010834
Sway only	0.010834
Initial bow only	0.010835

Table 5.3: Results of the load multiplier for the maximum load on the reference frame when imperfections are included in the beam element model.

As it can be seen in Table 5.3, the load multiplier for the maximum load of the reference frame is more or less the same whether or not imperfections are included. The displacement of the reference frame is, on the other hand, greater when imperfections are added. However, it is so that the calculation of $\alpha_{\text{ult,k}}$ refers to the load amplifier, which means that the results are based on the loads. As there is no change of maximum load at the yielding limit when imperfections are included, the imperfections are concluded not to be relevant for the reference frame. Hence, no imperfections are taken into account in this project report.

5.4.2 Determination of the Minimum Load Amplifier, $\alpha_{\text{cr,op}}$

The minimum load amplifier, $\alpha_{\text{cr,op}}$, is related to the out-of-plane behaviour of the reference frame. The determination of it is based on the eigenvalue problem described in Appendix F. The eigenvalue problem is shown in Eq. (5.3). The lowest eigenvalue, λ_{cr}, giving an out-of-plane buckling mode represents the minimum load amplifier, $\alpha_{\text{cr,op}}$, since the expression in Eq. (5.4) is valid and thereby, $\lambda_{\text{cr}} = \alpha_{\text{cr,op}}$.

$$([\mathbf{K}] + \lambda_{\text{cr}}\ [\mathbf{K}_\sigma]_{\text{ref}})\ \{\delta\ \mathbf{D}\} = \{\mathbf{0}\} \tag{5.3}$$

$$\alpha_{\text{cr,op}} = \frac{q_{\text{max}}}{q_{\text{actual}}} = \frac{\lambda_{\text{cr}}\ q_{\text{actual}}}{q_{\text{actual}}} \tag{5.4}$$

$[\mathbf{K}]$	Stiffness matrix	[-]
λ_{cr}	Eigenvalue - smallest level of external load for which there is bifurcation	[-]
$[\mathbf{K}_\sigma]_{\text{ref}}$	Stiffness matrix for stresses associated with load $\{\mathbf{R}\}_{\text{ref}}$	[-]
$\{\delta\ \mathbf{D}\}$	Eigenvector associated with λ_{cr} is the buckling mode (shown in Abaqus)	[-]

Abaqus/CAE is able to solve the eigenvalue problem in Eq. (5.3) and thereby show the lowest eigenvalue, λ_{cr}, giving an out-of-plane buckling mode. The lowest eigenvalue, λ_{cr}, is 2.8183 and thus is the minimum load amplifier, $\alpha_{\text{cr,op}} = 2.8183$ as well. It is the first buckling mode which gives this eigenvalue, and this buckling mode is shown in Figure 5.16.

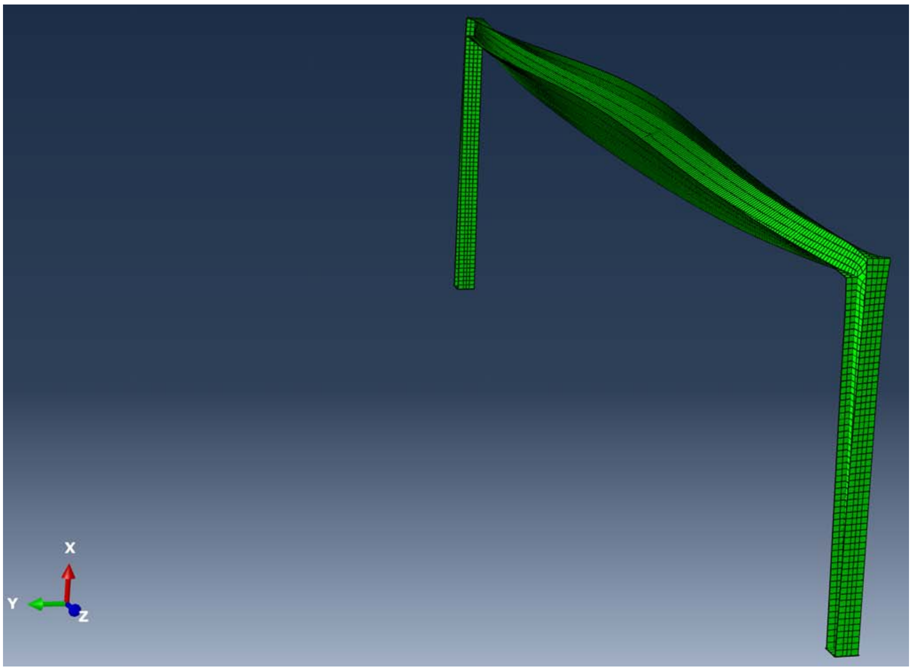

Figure 5.16: First buckling mode shown in 3D.

The first buckling mode shown in Figure 5.16 illustrates clearly that the reference frame buckles out-of-the-plane and lateral torsional buckling is present.

5.4.3 Determination of the Utilization Ratio, UR

To compare the results determined by the General Method to the results determined by Method 1, cf. Chapter 4, the utilization ratio, UR, is determined. This is done by the inverse of the General Method as shown in Eq. (5.5). The detailed calculation by the General Method is shown in Appendix G.

$$UR = \frac{1}{\frac{\chi_{op}\,\alpha_{ult,k}}{\gamma_{M1}}} \tag{5.5}$$

Firstly, the global non-dimensional slenderness, $\overline{\lambda}_{op}$, of a structural component for out-of-plane buckling has to be determined. This is done by the two minimum load amplifiers, $\alpha_{ult,k}$ and $\alpha_{cr,op}$, as shown in Eq. (5.6).

$$\overline{\lambda}_{op} = \sqrt{\frac{\alpha_{ult,k}}{\alpha_{cr,op}}} \tag{5.6}$$

$\alpha_{ult,k}$	Minimum load amplifier for in-plane behaviour, $\alpha_{ult,k} = 1.0378$	[-]
$\alpha_{cr,op}$	Minimum load amplifier for out-of-plane behaviour, $\alpha_{cr,op} = 2.8183$	[-]

Next, the value, Φ_{LT}, to determine the reduction factor, χ_{LT}, for lateral torsional buckling is calculated by Eq. (5.7).

$$\Phi_{LT} = 0.5\left[1 + \alpha_{LT}\left(\overline{\lambda}_{op} - \overline{\lambda}_{LT,0}\right) + \beta\,\overline{\lambda}_{op}^{2}\right] \tag{5.7}$$

α_{LT}	Imperfection factor for lateral torsional buckling, $\alpha_{LT} = 0.49$ (according to buckling curve c)	[-]
$\overline{\lambda}_{LT,0}$	Plateau length of the lateral torsional buckling curves for rolled sections, $\overline{\lambda}_{LT,0} = 0.4$ (Maximum value)	[-]
β	Correction factor for the lateral torsional buckling curves for rolled sections, $\beta = 0.75$ (Minimum value)	[-]

This value of Φ_{LT} is used to determine the reduction factor, χ_{LT}, for lateral torsional buckling in Eq. (5.8).

$$\chi_{LT} = \frac{1}{\Phi_{LT} + \sqrt{\Phi_{LT}^2 - \beta\,\overline{\lambda}_{op}^2}} \tag{5.8}$$

Hereafter, a value, Φ, to determine the reduction factor, χ, for lateral buckling is calculated in Eq. (5.9).

$$\Phi = 0.5\,\left[1 + \alpha\,\left(\overline{\lambda}_{op} - 0.2\right) + \overline{\lambda}_{op}^2\right] \tag{5.9}$$

α	Imperfection factor, $\alpha = 0.34$ (according to buckling curve b)	[-]

The result of Φ is used to determine the reduction factor, χ, for relevant buckling mode as shown in Eq. (5.10).

$$\chi = \frac{1}{\Phi + \sqrt{\Phi^2 - \overline{\lambda}_{op}^2}} \tag{5.10}$$

The reduction factor, χ_{op}, for the non-dimensional slenderness, $\overline{\lambda}_{op}$, can be determined by the minimum value of the reduction factor, χ_{LT}, for lateral torsional buckling and the reduction factor, χ, for lateral buckling as seen in Eq. (5.11).

$$\chi_{op} = \min \begin{cases} \chi_{LT} & \text{for lateral torsional buckling} \\ \chi & \text{for lateral buckling} \end{cases} \tag{5.11}$$

Finally, the utilization ratio, UR, can be determined by using Eq. (5.5), and this gives the utilization ratio, UR, shown in Table 5.4.

Model used to determine UR	UR
Beam Element Model	1.3870

Table 5.4: Utilization ratios, UR, determined by the General Method

The result in Table 5.4 shows that the reference frame is utilized over 100%. In Chapter 6, the utilization ratio, UR, is compared to the utilization ratios, UR, obtained by Method 1 in Chapter 4.

6 Comparison

This chapter gives a comparison between the utilization ratios, UR, determined by the analytical Interaction Formulae and by the numerical General Method both originating from Eurocode 3 [European Standard, 2005a]. In Table 6.1, the most critical utilization ratio, UR, determined by the Interaction Formulae and the utilization ratio, UR, determined by the General Method are shown.

Method	Utilization Ratio, UR
Interaction Formulae - y axis	1.09
General Method	1.387

Table 6.1: Comparison of utilization ratios, UR, determined by the Interaction Formulae and the General Method for the reference frame.

The highest utilization ratio, UR, determined by the Interaction Formulae is found in element 3 around the y axis which means that element 3 is the most critical element of the reference frame. It was not as expected since element 2 is four times longer than element 3 and is greatly exposed to the dominating snow load and thereby, would have been expected to be the most critical element.

As seen in Table 6.1, the General Method results in an even higher utilization ratio, UR, than the one determined by the Interaction Formulae. A way to interpret that could be that the General Method is more conservative than the Interaction Formulae. However, the expectation was that the General Method would give a more accurate result due to the use of the *Finite Element Analysis*, and that the Interaction Formulae would be the more conservative one, since this is based on simplifying assumptions. This is, unfortunately, not the case for the reference frame which is analysed in this project report.

To investigate the two methods additionally, a parameter study is conducted in the following Chapter 7.

7 Parameter Study

In order to investigate what happens due to instability if some input parameters are changed, a parameter study is done during the following chapter. The dimensions and material properties of the frame remain unchanged and the same applies to the supporting conditions at the bottom of element 1 and 3. However, the steel profile is changed from HE320A to IPE400, and additional fork supports is taken into account. In addition, the effect of a shear wall system is investigated by the Interaction Formulae. The calculations in this chapterare only shown for the changes made relative to the calculations done earlier in this project report.

7.1 Interaction Formulae - Shear Wall

This section will give the analytical solution of the the reference frame when the effect of shear wall is included. The calculation is done by a MATLAB code, which can be seen in Digital Appendix A.13 and A.14. An illustration of the effect of shear wall can be seen in Figure 7.1.

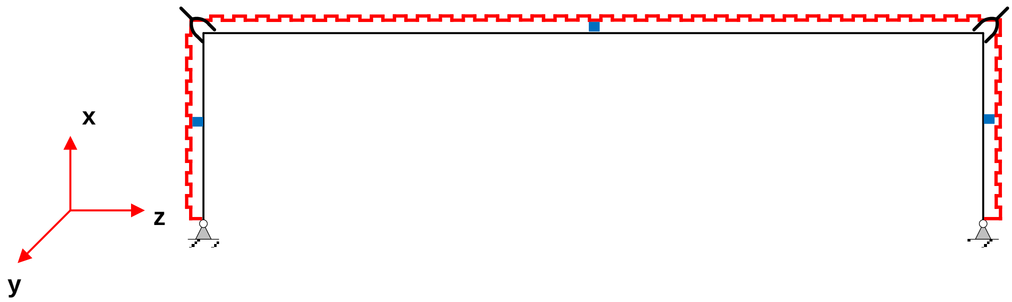

Figure 7.1: The reference frame with effect of shear wall

The effect of the shear wall on the reference frame comes to light when Method 1 is calculated. It is so that each element will be constrained along the top flanges, which mean that the elements are unable to move about the z-axis. This will effect the calculation of the reduction factor for the buckling mode, χ, and the reduction factor for lateral torsional buckling, χ_{LT}. However, the buckling length of the elements does not change. The calculations in this section will be according to what can be seen in Appendix B. However, only the results where there is a difference between the calculation of the reference frame and the reference frame when shear wall is included will be shown in this section.

7.1.1 Check of HE320A for Element 3

Buckling Curves

As for the reduction factor of buckling curve about the y axis, χ_y, there will be no difference. However, the reduction factor of buckling curve about the z axis, χ_z, will be equal to 1.0 as the frame is restrained to buckle about this axis.

Lateral Torsional Buckling Curves

For the calculation of the reduction factor for lateral torsional buckling, χ_{LT}, a new calculation must be made where the element is constrained. This means that m_6 needs to be found in order to calculate M_{cr}. The value for m_6 can be found based on the table in Figure 7.2.

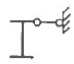

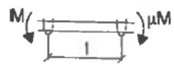

m_6

μ	kl = 0	1	2	3	4	6	8	10	15	20
1,0	4,93	5,18	5,93	7,18	8,93	13,9	20,9	29,9	61,2	105
0,5	6,53	6,86	7,84	9,48	11,8	18,2	27,1	38,3	76,0	127
0	9,28	9,73	11,0	13,2	16,1	24,2	34,7	47,5	89,0	144
−0,5	14,0	14,6	16,2	18,8	22,3	31,4	43,0	56,9	101	159
−1,0	20,8	21,4	23,2	26,0	29,7	39,4	51,9	66,7	114	175
−2,0	37,9	38,5	40,4	43,3	47,3	58,0	71,8	88,3	140	207
−4,0	83,9	84,6	86,5	89,7	94,0	106	121	140	200	275

Figure 7.2: Table 6 for an Eulerload [Mohr and et al., 2009].

In Figure 7.2, $\mu = 0$ and kl have been inserted. Based on this, a linear interpolation is made which gives a $m_6 = 12.386$. This will in the end result in $\chi_{LT} = 1.0$.

Results of Analytical Solution for element 3 of Shear Wall

Description	Value	Unit
Utilization of equation (4.1)	1.09	[-]
Utilization of equation (4.2)	0.64	[-]

Table 7.1: The results for method 1 for element 3 of HE320A including shear wall.

7.1.2 Check of HE320A for Element 2

Buckling Curves

The reduction factor of buckling curve, χ will be the same for element 2 as for element 3. This means that the reduction factor of buckling curve about the y axis, χ_y, will be the same as for the reference frame. However, the reduction factor of buckling curve about the z axis, χ_z, will be equal to 1.0 as the frame is restrained to buckle about this axis.

Lateral Torsional Buckling Curves

For the calculation of the reduction factor for lateral torsional buckling, χ_{LT}, a new calculation must be made where the element is constrained. This means that m_8 needs to be found in order to calculate M_{cr}. The value for m_8 can be found based on the table in Figure 7.3.

m_8										
	kl									
μ	0	1	2	3	4	6	8	10	15	20
$^1/_{24}$	1470	1489	1546	1639	1763	2093	2514	3012	4550	6471
$^1/_{16}$	385	397	434	492	569	765	1011	1299	2192	3319
$^1/_{12}$	168	175	198	233	281	409	572	767	1377	2159
$^1/_8$	71,7	75,2	85,8	103	127	195	285	396	759	1234

Figure 7.3: Table 8 for an Eulerload [Mohr and et al., 2009].

In order to use Figure 7.3, the two different end moments are split up and a m_8 for both end moments are calculated. The results can be seen in Table 7.2.

End moment	m_8	χ_{LT}
286.31 kNm	1224.0	1.0
309.89 kNm	1078.53	1.0

Table 7.2: The results for the reduction factor for lateral torsional buckling, χ_{LT}.

Results of Analytical Solution for element 2 of Shear Wall

Description	Value	Unit
Utilization of equation (4.1)	0.87	[-]
Utilization of equation (4.2)	0.49	[-]

Table 7.3: The results for method 1 for element 2 of HE320A including shear wall.

7.2 Interaction Formulae - Additional Fork Supports

This section will give the analytical solution of the the reference frame when the elements are supported with fork supports. An illustration of the fork supports can be seen in Figure 7.4.

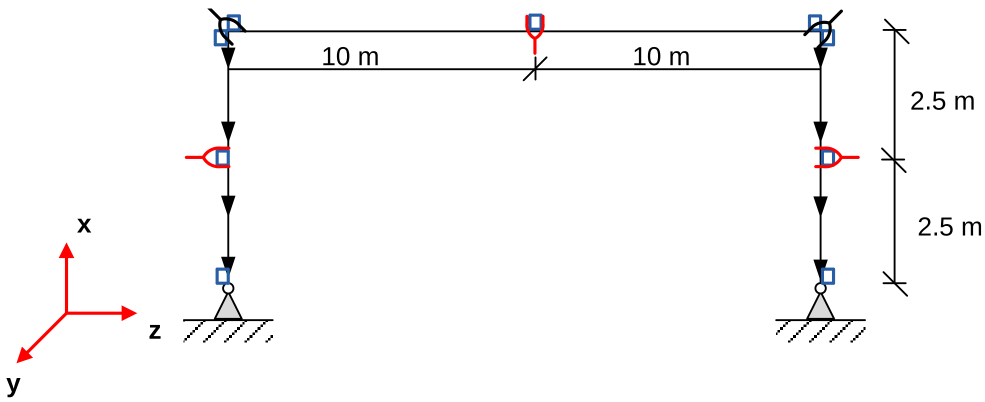

Figure 7.4: The reference frame with fork supports.

The effect of additional fork supports on the reference frame can be seen when the Interaction Formulae is calculated. The main effect of the additional fork supports is in regard of the the buckling length for lateral torsional buckling. In this case, the fork supports will influencing the reduction factor for lateral torsional buckling, χ_{LT}.

The load scenario for the frame is altered from line load to point load as illustrated in Figure 7.5. The line load will in this case be concentrated at the laths and purlin, giving point loads where these are placed on the frame. However, the self-weight is still calculated as a line load for each element. It should also be noticed that the self-weight of the laths and purlin are not taken into consideration for this section.

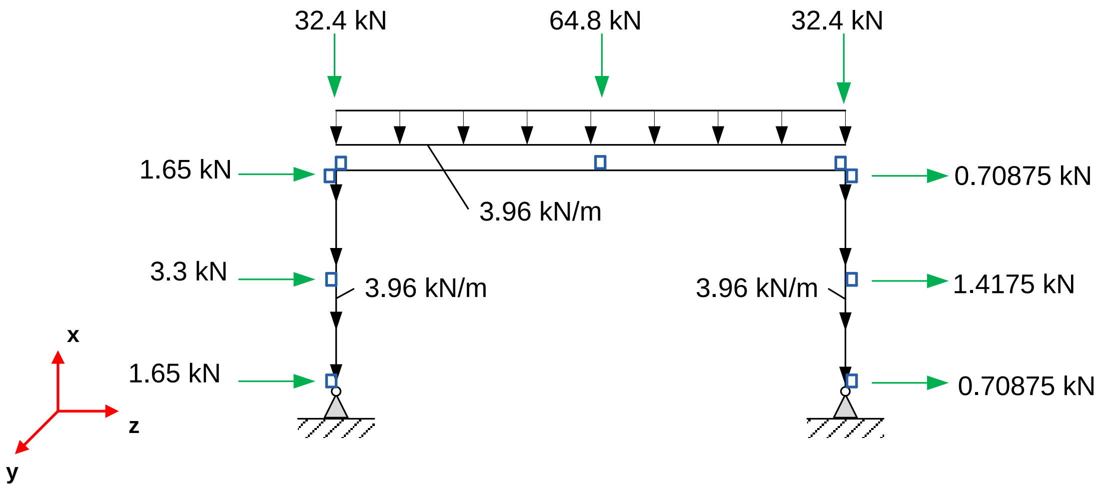

Figure 7.5: The new loads on the frame.

The calculations in this chapter will be according to what can be seen in Appendix B. However, only the results where there is a difference between the calculation of the reference frame and the reference frame when additional fork supports are applied is included will be shown in this section.

7.2.1 Forces and Moments

The new load distribution on the reference frame gives the following values used in the further calculations, see Table 7.4.

N_{Ed} elem. 3	$M_{\mathrm{y,Ed}}$ elem. 3	V_{Ed} elem. 3	N_{Ed} elem. 2	$M_{\mathrm{y,Ed}}$ elem. 2	V_{Ed} elem. 2
136.79 kN	285.34 kNm	58.48 kN	58.48 kN	285.34 kNm	136.79 kN

Table 7.4: The new forces and moments when purlins are taken into account for the reference frame.

The new moment distribution is illustrated in Figure 7.6.

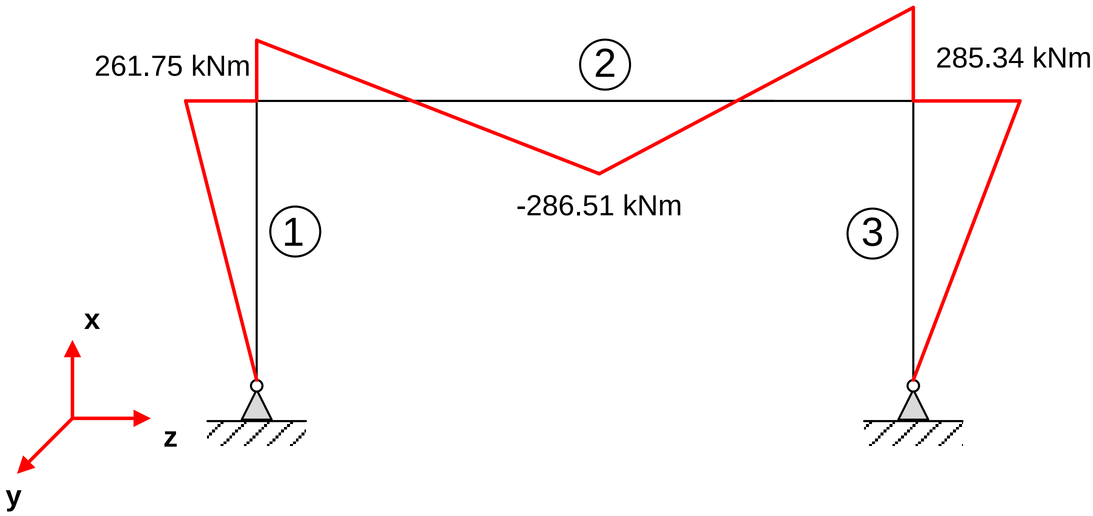

Figure 7.6: Illustration of the new moments occurring on the frame.

7.2.2 Check of HE320A for Element 3

Any elaboration of how the different parameters of the calculation are calculated is found in Appendix B.

Linear summation of the utilization ratios: Only one cross-section will be performed. This check can be seen in Eq. (7.1) and is calculated in the following equation shown in Eq. (7.2). The reason for not taking other checks is based on the results from the previous calculations of the reference frame found in Appedix B. The experience from here shows that Eq. (7.1) is the most critical one.

$$\frac{N_{\mathrm{Ed}}}{N_{\mathrm{Rd}}} + \frac{M_{\mathrm{y,Ed}}}{M_{\mathrm{y,Rd}}} + \frac{M_{\mathrm{z,Ed}}}{M_{\mathrm{z,Rd}}} \leq 1.0 \tag{7.1}$$

$$\frac{136.79 \text{ kN}}{2515.35 \text{ kN}} + \frac{285.34 \text{ kNm}}{347.8 \text{ kNm}} + 0 \leq 1.0 \tag{7.2}$$

$$0.87 \leq 1.0 \Rightarrow \text{OK}$$

For further details about the cross-section check, see Appendix B.

Buckling Curves

As for the reduction factor of buckling curve about the y axis, χ_{y}, there will be no difference from the reference frame as it may buckle about the same length. However, the reduction factor of buckling curve about the z axis, χ_{z}, change. The effective length will for the additional fork supports case have en effective length equal to $h/2$ (where h is equal to the height of the frame). When looking at the support condition for element 3, it is assumed that when the additional fork support is applied, the element will be fixed. Hence, the effective length is calculated for an element with pinned and fixed supports giving $l_{\mathrm{s}} = 0.7 \cdot 2500$ mm $= 1750$ mm. The effective length, $l_{\mathrm{s}} = 1750$ mm gives the following results shown in Table 7.5.

Effective length, l_s [mm]	$N_{cr,z}$ [kN]	χ_z [-]
1750	47239.0	0.979

Table 7.5: Calculation of the reduction factor of buckling curve, χ_z, when additional fork supports are used
.

Lateral Torsional Buckling Curves

For the calculation of the reduction factor for lateral torsional buckling, χ_{LT}, a new calculation must be made where the lateral torsional buckling length is assumed to be $h/2$ (where h is equal to the height of the frame). In addition, the element will not be constrained, meaning that table m_1 from Mohr and et al. [2009] will be used as shown in Figure 7.7.


m_1

$$m_1 = (9{,}22 - 4{,}29\,\mu)\sqrt{1 + \left(\frac{kl}{\pi}\right)^2}$$

$-1 \le \mu \le 1$

Figure 7.7: The Euler load for m_1 [Mohr and et al., 2009].

In order to use Figure 7.7, the relationship kl is calculated based on l = 2500 mm. μ is set to zero as there are no moments at the supports of the frame. The moment in the element can be seen i Table 7.4. The reduction factor for lateral torsional buckling, χ_{LT}, is calculated with the results shown in Table 7.6.

kl [-]	m_1 [-]	M_{cr} [kNm]	χ_{LT}
1.31	13.06	9020.3	1.0

Table 7.6: Calculation of the reduction factor for lateral torsional buckling, χ_{LT}, when additional fork supports are used .

Results of Analytical Solution of Additional Fork Supports

In Table 7.7, the utilization ratio of Eq. (4.1) and (4.2) is shown.

Description	Value	Unit
Utilization of equation (4.1)	1.03	[-]
Utilization of equation (4.2)	0.60	[-]

Table 7.7: The utilization ratio for Interaction Formulae for element 3 of HE320A including additional fork supports.

7.2.3 Check of HE320A for Element 2

Any elaboration of how the different parameters of the calculation are calculated is found in Appendix B.

Linear summation of the utilization ratios: Only one cross-section will be performed. This check can be seen in Eq. (7.1) and is calculated in the following equation shown in Eq. (7.4). The reason for not taking other checks is based on the results from the previous calculations of the reference frame found in Appedix B. The experience from here shows that Eq. (7.3) is the most critical one.

$$\frac{N_{\text{Ed}}}{N_{\text{Rd}}} + \frac{M_{\text{y,Ed}}}{M_{\text{y,Rd}}} + \frac{M_{\text{z,Ed}}}{M_{\text{z,Rd}}} \leq 1.0 \tag{7.3}$$

$$\frac{58.48 \text{ kN}}{2515.35 \text{ kN}} + \frac{285.34 \text{ kNm}}{347.8 \text{ kNm}} + 0 \leq 1.0 \tag{7.4}$$

$$0.84 \leq 1.0 \Rightarrow \text{OK}$$

For further details about the cross-section check, see Appendix B.

Buckling Curves

As for the reduction factor of buckling curve about the y axis, χ_y, there will be no difference from the reference frame as it may buckle about the same length. However, the reduction factor of buckling curve about the z axis, χ_z, change. The effective length will for the additional fork supports case have en effective length equal to $w/2$ (where w is equal to the width of the frame). When looking at the support condition for element 2, it is assumed that when the additional fork support is applied, the element will be fixed. Hence, the effective length is calculated for an element with pinned and fixed supports giving $l_s = 0.7 \cdot 1000$ mm $= 7000$ mm. The effective length, $l_s = 7000$ mm gives the following results shown in Table 7.8.

Effective length, l_s [mm]	$N_{cr,z}$ [kN]	χ_z [-]
7000	2952.4	0.56

Table 7.8: Calculation of the reduction factor of buckling curve, χ_z, when additional fork supports are used

.

Lateral Torsional Buckling Curves

For the calculation of the reduction factor for lateral torsional buckling, χ_{LT}, a new calculation must be made where the lateral torsional buckling length is assumed to be $w/2$ (where w is equal to the width of the frame). In addition, the element will not be constrained. The moment distribution of element 2 is illustrated in Figure 7.6, where it can be seen that the moment distribution is mainly from the point loads on the element. This means that table m_1 from Mohr and et al. [2009] will be used as shown in Figure 7.8.

Figure 7.8: The Euler load for m_1 [Mohr and et al., 2009].

In order to use Figure 7.8, the relationship kl is calculated based on l = 10000 mm. μ is calculated from the relatioship of the end moment and the moment in the middle of the element, see Eq. (7.5).

$$\mu = \frac{285.34 \text{ kNm}}{-286.51 \text{ kNm}} = -0.9959 \tag{7.5}$$

By inserting μ = -0.9959 and the relationship kl, the reduction factor for lateral torsional buckling, χ_{LT}, is calculated with the results shown in Table 7.9.

kl [-]	m_1 [-]	M_{cr} [kNm]	χ_{LT}
5.25	22.05	951.85	0.95

Table 7.9: Calculation of the reduction factor for lateral torsional buckling, χ_{LT}, when additional fork supports are used .

Results of Analytical Solution of Additional Fork Supports

In Table 7.10, the utilization ratio of Eq. (4.1) and (4.2) is shown.

Description	Value	Unit
Utilization of equation (4.1)	0.85	[-]
Utilization of equation (4.2)	0.49	[-]

Table 7.10: The utilization ratio for Interaction Formulae for element 2 of HE320A including additional fork supports.

7.3 Interaction Formulae - Change of Profile to IPE500

This section will calculate the reference frame and the previously parameter study conducted for shear wall effect and additional forks supports, with a new profile, IPE500. All of the assumptions and calculations are the same as seen in Section 4.4, 7.1 and 7.2 except for the normal force and the moment which will be lower because of a reduction of the self-weight. This section will, however, only give the final utilization ratio for each case.

7.3.1 Reference frame - IPE

The utilization ratio for element 3 and 2 can be seen in Table 7.11 and 7.12, respectively.

Description	Value	Unit
Utilization of equation (4.1)	0.77	[-]
Utilization of equation (4.2)	0.54	[-]

Table 7.11: The results for Interaction Formulae for element 3 of IPE500 for the reference frame.

Description	Value	Unit
Utilization of equation (4.1)	0.55	[-]
Utilization of equation (4.2)	0.97	[-]

Table 7.12: The results for Interaction Formulae for element 2 of IPE500 for the reference frame.

7.3.2 Effect of Shear Wall - IPE

The utilization ratio for element 3 and 2 can be seen in Table 7.13 and 7.14, respectively.

Description	Value	Unit
Utilization of equation (4.1)	0.80	[-]
Utilization of equation (4.2)	0.49	[-]

Table 7.13: The results for Interaction Formulae for element 3 of IPE500 for the effect of shear wall.

Description	Value	Unit
Utilization of equation (4.1)	0.53	[-]
Utilization of equation (4.2)	0.31	[-]

Table 7.14: The results for Interaction Formulae for element 2 of IPE500 for the effect of shear wall.

7.3.3 Additional Fork Supports - IPE

The utilization ratio for element 3 and 2 can be seen in Table 7.15 and 7.16, respectively.

Description	Value	Unit
Utilization of equation (4.1)	0.7	[-]
Utilization of equation (4.2)	0.44	[-]

Table 7.15: The results for Interaction Formulae for element 3 of IPE500 for the additional fork supports.

Description	Value	Unit
Utilization of equation (4.1)	0.62	[-]
Utilization of equation (4.2)	0.44	[-]

Table 7.16: The results for Interaction Formulae for element 2 of IPE500 for the the additional fork supports.

7.4 General Method - Shear Wall

The reference frame is in this section modified to the configuration shown in Figure 7.9, where an effect of a shear wall system is present. A purlin is placed on the upper flange on element 2 while laths are placed on the outer flanges on element 1 and 3, respectively. These out-of-plane elements are used as supports for the cladding and to stabilize the frame out-of-the-plane.

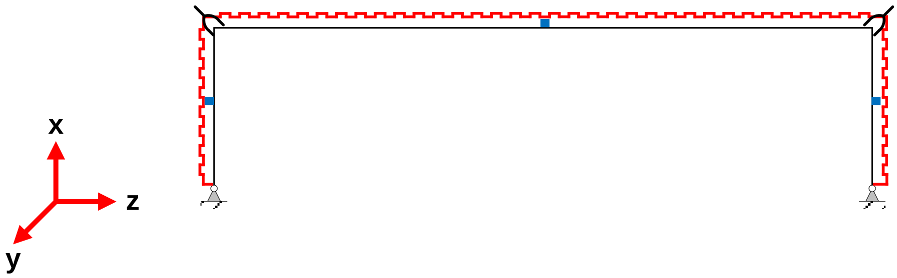

Figure 7.9: Effect of shear wall system.

To model this configuration in *Abaqus/CAE*, the boundary conditions and loads are changed compared to what is done on the reference frame. The pinned support conditions and the fork supports in the corners of the frame are still applied but now the frame is out-of-plane supported at the midpoints of the elements. This means that in these points $U_y = 0$. Additionally, the rotation around the z axis, U_{Rz}, is fixed and thereby equal to zero at the midpoints of element 1 and 3 while the rotation around the x axis, U_{Rx}, is fixed and thereby equal to zero at the midpoint of element 2. Because of these out-of-plane elements, the loading conditions are changed from uniformly distributed surface loads acting on the outer flanges to point loads acting at the pinned supports, the midpoints and the corners of the frame. The loads are shown in Figure 7.5.

The General Method is used to determine the utilization ratio, UR, of this configuration. The General Method is described in Chapter 5 and a worked example is shown in Appendix G. The results of an analysis of this configuration are shown in Table 7.17.

Description	Symbol	Value	Unit
Minimum load amplifier related to in-plane behaviour	$\alpha_{\text{ult,k}}$	0.6757	[-]
Minimum load amplifier related to out-of-plane behaviour	$\alpha_{\text{cr,op}}$	1.4975	[-]
Utilization ratio	UR	2.2215	[-]

Table 7.17: Minimum load amplifiers, $\alpha_{\text{ult,k}}$ and $\alpha_{\text{cr,op}}$, related to in-plane and out-of-plane behaviour, respectively, and utilization ratio, UR, for frame with effect of shear wall system.

As seen in Table 7.17, this configuration results in an even larger utilization ratio, UR, than the reference frame. Therefore, there must be an error somewhere, since this configuration should be more stable and thereby less utilized than the reference frame.

7.5 Discussion

From the analytical parameter study conducted, the worst case for an element with HE320A profile turned out to be the reference frame and the reference frame when shear wall is included. The highest utilization ratio was 1.09 (109 %) for element 3. The reason for the worst case being both the reference frame and the reference frame when shear wall is included is due to the critical moment, M_{cr}. The critical moment will result in a reduction factor for lateral torsional buckling, $\chi_L T$ of 1.0 for both cases. For the General Method, the effect of shear wall gave a utilization ratio of 2.22 (222%), which is significantly higher than expected. It would be assumed that the analytical method would be more conservative, and that the General Method would give the lowest utilization ratio due to the use of *Finite Element Analysis*.

In regard of the parameter study for an element with IPE 500 profile, the worst case is for the reference frame about the z axis for element 2. This is most likely due to sectional properties about the z axis, meaning that for an element length of 20 m, the z axis will become critical.

For the analytical parameter study it can be said that the reference frame will for all cases be the most critical by having the highest utilization ratio. As the elements are supported by additional fork supports, the utilization ratio decrease as suspected.

8 Conclusion

The goal of this master thesis has been to investigate a predefined reference frame for instability by two different methods given in Eurocode 3 [European Standard, 2005a]. The first one - the Interaction Formulae - determines directly the utilization ratio, UR, of an element subjected to combined bending and axial compression around both the y and z axis. The method takes into account instability effects such as buckling and lateral torsional buckling, and it is highly dependent on how the supporting conditions are assumed.

The Interaction Formulae shows a utilization ratio, UR, of 1.09 (109%) around the y axis of element 3. This means that for the reference frame, element 3 will be the critical element. The results shows that buckling effects are critical due to the slenderness of the section. However, lateral torsional buckling effects are not critical for this element.

The second method to investigate a frame for instability is the General Method which allows to make use of a *Finite Element Analysis* to determine two minimum load amplifiers, $\alpha_{\mathrm{ult,k}}$ and $\alpha_{\mathrm{cr,op}}$, related to the in-plane and out-of-plane behaviour of a frame, respectively. The utilization ratio, UR, determined by the General Method is unfortunately higher than the one determined by the Interaction Formulae. The General Method results in a utilization ratio, UR, of 1.3870 (139%).

A way to interpret that the utilization ratio, UR, is higher determined by the General Method compared to the Interaction Formulae could be that the General Method is more conservative than the Interaction Formulae. However, the expectation was that the General Method would give a more accurate result due to the use of the *Finite Element Analysis*, and that the Interaction Formulae would be the more conservative one, since this is based on simplifying assumptions. This is, unfortunately, not the case for the reference frame which is analysed in this master thesis. In the parameter study for the Interaction Formulae, the utilization ratio of element 2 is found to be the worst case with a value of 0.97 (97%) about the z axis for the reference frame by using an IPE500 steel profile. It can aslo be seen from the parameter study that the additional fork supports on the frame will help to stabilize and in the end giving a smaller utilization ratio for the frame.

8.1 Further Studies

There are a number of different parameters which are well suited for an analysis of a frame, but because of the extent and complexity of frame, only some parameters has been chosen. However, there are further studies that can be made in order to investigate a steel frame. Some of these further studies are listed below:

- In a further investigation of a steel frame, the support conditions could be altered to fixed supports to see what effect that would have on the stability of the frame by using the Interaction Formulae and the General Method.
- The angle of the roof could have been varied in order to investigate how a pitched-roof frame would behave according to the Interaction Formulae and the General Method.
- From the literature study, articles shows that the stability of the frame is very depending on how the joints of the frame is modeled. This will have a great impact on the stability of the frame, and it would therefore be interesting to investigate further.

- The cross-section of the frame could be made with a non constant cross-section in order to see how the General Method would analyse the stability the frame.

Bibliography

Andersen and Petersen, 2010. Ulrik Andersen and Stefan Petersen. *Bygningsingeniør: Halvdelen af undersøgte tage har fejl - 6.000 tage bør tjekkes*. URL: `http://kortlink.dk/c3q7`, 2010. Downloaded: 15-02-2013.

Autobaler. Autobaler. *Portal Frame Buildings*. URL: `http://kortlink.dk/cewp`. Downloaded: 05-04-2013.

Bonnerup and et al., 2009. Bent Bonnerup and et al. *Stålkonstruktioner efter DS/EN 1993*. Nyt Teknisk Forlag, 1. edition, 2009. ISBN 978-87-571-2683-9.

BYG-ERFA. BYG-ERFA. *Forstærkning af simple stålrammebygninger*. URL: `https://kortlink.dk/a99e`. Downloaded: 04-04-2013.

Connections.org. Connections.org. *Flexural-Torsional Buckling*. URL: `http://kortlink.dk/cews`. Downloaded: 13-05-2013.

Silva and et al, 2010. Luís Simões da Silva and et al. *Design of Steel Structures, Eurocode 3: Design of steel structures. Part 1-1: General rules and rules for buildings*. ECCS - European Convention for Constructional Steelwork, 2010.

Eurocode-resources.com. Eurocode-resources.com. *Buckling*. URL: `http://kortlink.dk/cewn`. Downloaded: 04-04-2013.

European Standard, 2005a. European Standard. *Eurocode 3: Design of Steel Structures - Part 1-1: General Rules and Rules for Buildings*. European Standard, 2005.

European Standard, 2005b. European Standard. *Eurocode 0: Basic of Structural Design*. European Standard, 2005.

European Standard, 2002. European Standard. *Eurocode 1: Actions on structures - Part 1-1: General actions - Densities, self-weight, imposed loads for buildings*. European Standard, 2002.

European Standard, 2007a. European Standard. *Eurocode 1: Actions on structures - Part 1-3: General actions - Snow loads*. European Standard, 2007.

European Standard, 2007b. European Standard. *Eurocode 1: Actions on structures - Part 1-4: General actions - Wind actions*. European Standard, 2007.

Freedom Steel, 2010. *Freedom Steel*. URL: `http://kortlink.dk/chfm`, 2010. Downloaded: 02-06-2013.

Lett-Tak Systemer AS. Lett-Tak Systemer AS. *Lett-Tak*. URL: `http://kortlink.dk/cewg`. Downloaded: 06-05-2013.

Ljubljana University, a. Ljubljana University. *Lecture 6.3: Elastic Instability Modes*. URL: `http://kortlink.dk/cewm`. Downloaded: 04-04-2013.

Ljubljana University, b. Ljubljana University. *Lecture 6.6.2: Buckling of Real Structural, Elements II*. URL: `http://kortlink.dk/cewk`. Downloaded: 04-04-2013.

Made-in-China.com. *Made-in-China.com*. URL: `http://kortlink.dk/chfn`. Downloaded: 02-06-2013.

Mohr and et al., 2009. Gunnar Mohr and et al. *Teknisk Ståbi*. Nyt Teknisk Forlag, 20. edition, 2009. ISBN 978-87-571-2685-3.

SIMULIA, 2012. SIMULIA. *Getting Started with Abaqus: Interactive Edition*, 2012.

Solberg, 2011. Andreas Solberg. *Historiske kollapser de siste 10 år*. URL: `http://kortlink.dk/c3q6`, 2011. Downloaded: 15-02-2013.

Steltech-Structural. Steltech-Structural. *Portal Frame Buildings*. URL: `http://kortlink.dk/cewq`. Downloaded: 05-04-2013.

Wikipedia. Wikipedia. *Column*. URL: `http://kortlink.dk/cewr`. Downloaded: 16-04-2013.